

**“LIBS limit of detection and plasma parameters studies  
using single and double pulse configuration”**



*By*

**AYESHA MAHMOOD**

**Supervisor:**

**Dr. Shaista Shahzada**

Assistant Professor,

Department of Physics, FBAS, IIUI

**Co-Supervisor:**

**Dr. Sami-ul-Haq**

Principal Scientist,

NILOP Islamabad

**Department of Physics**

**Faculty of Basic and Applied Sciences**

**International Islamic University, Islamabad (2015)**



TH-16125  
Accession No           

K  
H. Hill

MS  
543.52  
AYL

**INTERNATIONAL ISLAMIC UNIVERSITY  
FACULTY OF BASIC AND APPLIED SCIENCES  
DEPARTMENT OF PHYSICS  
ISLAMABAD PAKISTAN  
(2015)**

**LIBS limit of detection and plasma parameters studies using single  
and double pulse configuration**

**By:**


**Ayesha Mahmood**

**(205-FBAS/MSPHY/F13)**

**This thesis is submitted to Department of Physics,  
International Islamic University Islamabad for the award of  
MS Physics degree.**

**Dr. Sharmila Sajjad**  
Chairperson  
Department of Physics (FBAS)  
International Islamic University  
Islamabad  
18/4/16

**(Chairperson, Department of Physics)**



**(Dean FBAS, IIU, Islamabad)**

**INTERNATIONAL ISLAMIC UNIVERSITY  
FACULTY OF BASIC AND APPLIED SCIENCES  
DEPARTMENT OF PHYSICS  
ISLAMABAD PAKISTAN  
(2015)**

**LIBS limit of detection and plasma parameters studies using single  
and double pulse configuration**

**By:**

**Ayesha Mahmood**

**(205-FBAS/MSPHY/F13)**

**This thesis is submitted to Department of Physics,  
International Islamic University Islamabad for the award of  
MS Physics degree.**

**Dr. Shamaila Sajjad**  
Chairperson  
Department of Physics (FC FBAS)  
International Islamic University  
Islamabad  
18/4/16

**(Chairperson, Department of Physics)**



**(Dean FBAS, IIU, Islamabad)**

**Faculty of Basic and Applied Sciences**

**Department of Physics**

**Dated: 03-12-2015**

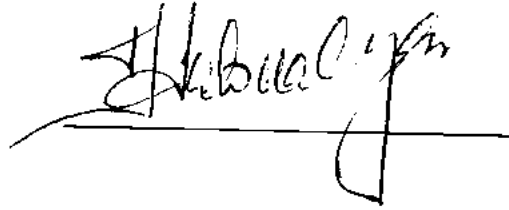
**Final Approval**

This is to certify that the work contained in this thesis entitled: "LIBS limit of detection and plasma parameters studies using single and doubled-pulse configuration" was carried out by **Ayesha Mahmood**, Registration number (205-FBAS/MSPHY/F-13) and in our opinion, it is fully adequate, in scope and quality, for the degree of M.S. Physics.

**Committee**

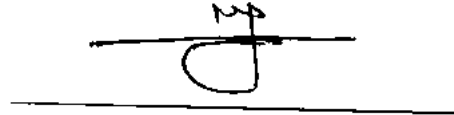
**External Examiner**

Dr. Muhammad Mazhar Ali Kalyar  
Assistant Professor, Department of Physics,  
University of Sargodha



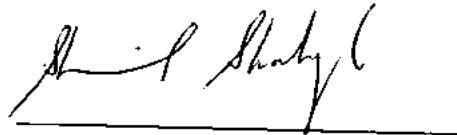
**Internal Examiner**

Dr. Naeem Ahmad  
Assistant Professor,  
Department of Physics, FBAS, IIUI



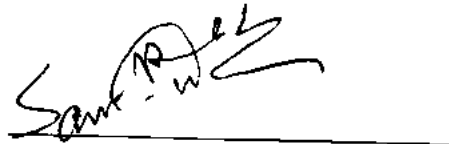
**Supervisor**

Dr. Shaista Shahzada,  
Assistant Professor,  
Department of Physics, FBAS, IIUI



**Co-Supervisor**

Dr. Sami-ul-Haq  
Principal Scientist,  
NILOP, Islamabad



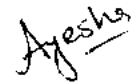
*A Thesis Submitted to the  
Department of Physics  
Faculty of Basic & Applied Sciences of IIUI  
In partial fulfillment of the Requirement  
For the degree of M.S. Physics*

بِسْمِ اللَّهِ الرَّحْمَنِ الرَّحِيمِ

## **Declaration of Originality**

I, hereby declare that the work presented in the thesis is my own work. This thesis has not been previously published in any form nor does it contain any verbatim of the published resources that could be treated as infringement of the international copyright law.

I also declare that I do understand the terms 'copyright' and 'plagiarism,' and that in case of any copyright violation or plagiarism found in this work, I will be held fully responsible of the consequences of any such violation.



**Ayesha Mahmood**

(205-FBAS/MSPHY/F-13)



## **Dedications**

This thesis is dedicated to my **parents & family** who have supported me all the way.

Finally, this thesis is dedicated to **all** those who believe in the richness of learning.

## Acknowledgements

First of all I am grateful to the **Almighty Allah** for His blessings and for establishing me to complete my work. Also, I would like to thank all those people who made this thesis possible and an unforgettable experience for me.

I would like to express my deepest sense of gratitude to my supervisor **Dr. Shaista Shahzada** who offered her continuous advice and encouragement throughout the course of this thesis.

I am thankful to my co-supervisor **Dr. Sami-ul-Haq** for providing me the best facilities related to my work, positive criticism and encouragement at all times. I would like to acknowledge **Dr. Ali Nadeem** for their valuable suggestions.

I avail the opportunity to pay special thanks to **Dr. Muhammad Rafi** who took great interest for the preparation of sample of my project.

I am very obliged to **Dr Mushtaq Ahmed** (Director of NILOP), who was very kind and provided me space in prestigious institute for timely accomplishment of my thesis.

I am also thankful to the scientists and staff of Laser spectroscopy laboratory at National Institute of Laser and Optronics (NILOP) for providing me the chance to work under the great environment.

I am grateful to my **parents** and **siblings** for their unconditional love and prayers.

*Ayesha*

**Ayesha Mahmood**

**HUI Islamabad**

# Table of contents

<b>Abstract</b> .....	1
<b>Introduction</b> .....	2
1.1 Laser Induced Breakdown Spectroscopy (LIBS).....	2
1.2 Historical Background of LIBS.....	2
1.3 Literature survey about limit of detection .....	3
1.4 Plasma .....	4
1.5 Laser matter interaction.....	4
1.6 Laser induced plasma .....	6
1.7 Temporal evolution of LIBS plasma .....	7
1.8 Conventional techniques .....	8
1.9 Broadening of spectral lines .....	8
1.9.1 Natural broadening.....	9
1.9.2 Doppler broadening .....	9
1.9.3 Stark Broadening .....	9
1.10 Determination of electron number density.....	10
1.11 Determination of plasma temperature .....	10
1.11.2 Plasma temperature using Intensity Ratio method.....	11
1.12 Local thermal equilibrium (LTE).....	11
1.13 Plasma opacity and self-absorption.....	12
1.14 Quantitative analysis using calibration curve.....	12
1.15 Limit of detection .....	13
1.16 Polymer and sample description .....	14
1.17 Double pulse LIBS .....	14
1.18 LIBS Applications.....	15
<b>Experimental Setup and Procedure</b> .....	16
2.1 Sample preparation.....	16
2.2 LIBS Instrumentation.....	17
2.2.1 Laser system.....	18
2.2.3 Beam focusing and collection system.....	20

2.2.4	Sample stage .....	20
2.2.5	LIBS-Spectrometer .....	21
2.2.6	LIBS software .....	24
2.2.7	Spectral Resolution .....	24
2.3	Experimental Procedure .....	25
<b>Experimental Results and Discussion .....</b>		<b>28</b>
3.1	Emission spectra of Silver Nitrate doped Polymer .....	28
3.1.1	Double pulse LIBS.....	31
3.2	Calibration Curves.....	35
3.3	Limit of detection .....	41
3.4	Study of plasma parameters .....	44
3.4.1	Plasma temperature.....	45
3.4.2	Electron Number Density .....	46
<b>Conclusion .....</b>		<b>48</b>
<b>Future Recommendations .....</b>		<b>48</b>
<b>References.....</b>		<b>49</b>

# List of Figures

<b>Figure 1.1</b> Schematic diagram of laser induced plasma.....	5
<b>Figure 1.2</b> (a) shows broadband emission due to bremsstrahlung and free bound transition, (b) shows line emission due to bound-bound transition.....	5
<b>Figure 1.3</b> A schematic diagram of the temporal history of a LIBS plasma.....	7
<b>Figure 1.4</b> Calibration curve concentration vs signal intensity.....	12
<b>Figure 1.5</b> Schematic representation of different double –pulse configuration (a) shows collinear, (b) orthogonal reheating.....	15
<b>Figure 2.1</b> Magnetic stirrer used for solution mixing.....	16
<b>Figure 2.2</b> Blank sample of PMMA inside patri dish.....	17
<b>Figure 2.3</b> Thin film sample of PMMA doped with different concentration of AgNO <sub>3</sub> .....	17
<b>Figure 2.4</b> Energy level diagram of the trivalent neodymium ion.....	19
<b>Figure 2.5</b> Laser beam profile, showing an intensity profile.....	19
<b>Figure 2.6</b> Formation of plasma plume.....	20
<b>Figure 2.7</b> Sample placed inside the sample chamber.....	21
<b>Figure 2.8</b> Seven channel LIBS 2500+ spectrometer.....	21
<b>Figure 2.9</b> LIBS spectrometer with components.....	22
<b>Figure 2.10</b> shows silicon based Charged Couple Device (CCD) consists of pixels which converts photons of light into electrons.....	23
<b>Figure 2.11</b> Clocking out of charges row wise.....	24
<b>Figure 2.12</b> LIBS setup.....	25
<b>Figure 2.13</b> Block diagram of collinear double pulse LIBS setup.....	26

<b>Figure 3.1</b> Portion of emission spectrum of silver nitrate doped polymer using single pulse LIBS at 120 mJ per pulse energy. The emission lines of Ag, Na, Ca, CN and C <sub>2</sub> are evident in the spectrum.....	29
<b>Figure 3.2</b> Portion of emission spectrum of polymer having spectral lines of silver using single pulse.....	30
<b>Figure 3.3</b> Portion of emission spectra of polymer having spectral lines of silver using single pulse.....	30
<b>Figure 3.4</b> Variation in signal intensities of three lines 308.24 nm, 358.7 nm, 394.4 nm at different inter pulse delay.....	32
<b>Figure 3.5</b> Variation in signal intensity as a function of energy ratio.....	33
<b>Figure 3.6</b> Double pulse emission spectra of polymer.....	34
<b>Figure 3.7</b> Comparison of signal intensity on using single and double pulse.....	35
<b>Figure 3.8</b> Calibration curve showing all data points from 1000-0.30 µg/ml concentration of transition of Ag in polymer.....	37
<b>Figure 3.9</b> (a) and (b) shows calibration curves of Ag (328.06 nm and 546.55 nm) in polymer using single pulse.....	38
<b>Figure 3.10</b> (a)-(d) shows Calibration curve for Silver (Ag) transition 328.06 nm, 338.28 nm, 520.91 nm and 546.55 nm respectively applying double pulse.....	40
<b>Figure 3.11</b> Measurement on standard along with blank measurement.....	41
<b>Figure 3.12</b> Emission spectra of blank sample showing no transition line at 328.06, 338.28, 520.91 and 546.55 nm (Ag lines).....	43
<b>Figure 3.13</b> Typical Silver emission line (328.06 nm), fitted with Lorentzian function. ....	47

## List of Tables

<b>Table 2.1</b> Specifications of Nd: YAG laser.....	18
<b>Table 3.1</b> composite and percentage concentration of reference samples is given below.....	36
<b>Table 3.2</b> Chosen emission lines and their spectroscopic data for various element is given for single pulse.....	42
<b>Table 3.3</b> Chosen emission lines and their spectroscopic data for various element is given for double pulse.....	44
<b>Table 3.4</b> Spectroscopic parameters of the observed silver lines used in order to determine the plasma temperature.....	45

## Abstract

In the present work, laser induced breakdown spectroscopy (LIBS) technique has been used to find out the limit of detection and improvement in limit of detection using double pulse configuration. The reference samples were prepared by mixing known concentration solution of silver nitrate ( $\text{AgNO}_3$ ) in polymer polymethyl methacrylate (PMMA). In the polymer PMMA, the concentration of  $\text{AgNO}_3$  has been varied from 1000  $\mu\text{g/ml}$  to 0.24  $\mu\text{g/ml}$  using solvent casting method and the plasma of thin film has been produced using fundamental harmonic (1064 nm) of Nd: YAG laser at energy 120 mJ, at atmospheric pressure in air using single pulse. The emission spectra of all the samples were recorded through LIBS 2500+ spectrometer (Ocean Optics Inc.) having spectral range 200-980 nm and spectral resolution 0.1 nm. The emission spectra have been analyzed and two emission lines of silver at 328.06 nm and 546.55 nm have been selected to find the limit of detection. For that purpose, calibration curves were constructed using line emission intensities from reference samples. The slope of the calibration curves and the standard deviation of the blank sample has been used which yield the limit of detection as 10 and 19  $\mu\text{g/ml}$  for single pulse LIBS.

Similarly the emission spectra of reference sample have been recorded using double pulse LIBS in collinear configuration. The spectra were recorded under optimized experimental condition by fixing inter-pulse delay to 5  $\mu\text{s}$  and energy ratio of both lasers equal to 1:1. The recorded emission spectra have been analyzed and four silver lines have been used for the construction of calibration curves. The slope from the calibration curves and standard deviation from blank samples yield the limit of detection as approximately 6  $\mu\text{g/ml}$ . The limit of detection is almost two times improved as compared to single pulse LIBS.

In addition, plasma temperature has been extracted using intensity ratio method and the electron number density has been estimated from the Stark broadening of silver line profile. At 120 mJ per pulse laser energy, the electron temperature is extracted as  $10,000 \pm 100$  K and number density as  $13.5 \times 10^{14} \text{ cm}^{-3}$ .



## Introduction

### 1.1 Laser Induced Breakdown Spectroscopy (LIBS)

Laser induced breakdown spectroscopy (LIBS) is an atomic emission spectroscopy which uses an intense laser pulse to produce optical sample excitation [1]. Laser irradiance must have greater than target threshold value typically  $10^9$ - $10^{10}$  Wcm<sup>-2</sup>, for generation of plasma consists of ionized matter [2]. Plasma consists of free electrons ionic and neutral species but as a whole it is electrically neutral. The plasma spread in each direction but its expansion towards laser beam is more than other directions. As a result plasma cools down and the excited and ionized species de-excite or recombine and release their energy. The excited species emit radiations which is used for the measurement of plasma parameters and for analytical applications. After that plasma light allow falling on spectrometer through fiber, to capture the emission which gives a spectrum for analysis. The emission spectra can be analyzed using references such as Army Research Laboratory (ARL) and National Institute of Standards and Technology (NIST) of atomic spectra database [3, 4]. LIBS gives both qualitative and quantitative analysis. Qualitative analysis gives information about the existence of elements in the sample and quantitative analysis gives information about the amount of element present in the sample. LIBS can detect trace element in parts per million (ppm). Sample may be solid, liquid or aerosol. LIBS is an easy setup and has an advantage of little or no sample preparation. Using Nd: YAG laser with Q-switching operation, make it valuable. LIBS is used to study the pollution in environment, compositional analysis of different metals, and its use in nuclear industry is of worth importance. It has also industrial applications in defense field to detect trace element of explosives.

### 1.2 Historical Background of LIBS

In 1960, with the invention of laser, history of laser matter interaction starts. Work on laser induced breakdown spectroscopy starts after the invention of pulsed Ruby laser [2]. After that Brech and Cross [5], using laser for atomic excitation and create plasma in solid, liquid and in air. Gue'don and Liodee [6] reported the analytical use of LIBS for the spectrochemical analysis of surface. Maker et al. [7] observed optically induced breakdown in gases. In the same year Runge et al. [8] observed the use of pulsed Q- switch ruby laser for direct spark excitation on metals. The

comparison between Q switched and continues lasers for ablation of material reported by Scot and Strashiem [9]. The breakdown in gases was studied by physicists in 1971 [10] to understand the phenomena. The work in air can be found in 1980s [11, 12]. Laser spark spectrochemical analysis of liquids was done by generating plasma on the surface or inside of liquid [13]. Wachter et al. [14] analyzed the emission spectra of uranium in the form of solution in nitric acid. In 1980s for analyzing soil contamination and lead in paint Alamos et al. [15] constructed a beryllium monitor. The analysis of salt concentration in sea water was reported by Alexander [16]. Second harmonic of a pulsed Nd: YAG laser was used by Milan and Laserna [17] for the ablation of silicon sample in air at atmospheric pressure. Ismail et al. [18] studied the plasma parameter and LOD of some elements present in two different metallic matrices. Shaikh et al. [19] studied the visible emission spectroscopy from a tin sample in vacuum using a CO<sub>2</sub> laser. In the same year Emily and Almirall [20] studied the unprocessed cotton for determination of the elemental profile major, minor and trace element present in the unprocessed cotton. In the year 2000, many advancement was made in LIBS in instrumentation and like photodiode array (PDA), charged couple device (CCD) and intensified charged couple device (ICCD) and their applications.

### 1.3 Literature survey about limit of detection

Laser induced breakdown spectroscopy (LIBS) technique is used for qualitative, quantitative analysis and to find limit of detection (LOD) using samples with known concentration of species. Qualitative analysis tells the presence of an element in the sample and limit of detection gives the least concentration that the system can detect. LOD also depends on spectral resolution of spectrometer. With single pulse, limit of detection is poor and its sensitivity can be improved by using double pulse configuration with optimized parameters. Aguilera et al. [21] determined carbon contents in steel by focusing laser pulse of 200 mJ in nitrogen atmosphere and obtained the limit of detection 65 ppm with 1.6 % uncertainty. Improvement in limit of detection and enhancement in signal intensities is possible by the use of double pulse configuration [22, 23]. Detection limit for different element in steel were less than 10 µg/g with collinear double pulse [24]. Marva et al. [25] investigate limit of detection for different elements in aluminum and steel alloy at atmospheric pressure at 120 mJ per pulse energy in single and double pulse. Marva et al. [26] study matrix effect in limit of detection and limit of detection of Mg, Si, Mn and Cu as trace element was found in aluminum standard samples alloys using single pulse by focusing 70mJ of

laser pulse at 1064 nm with 7 ns duration and compare it with the values of same elements in steel alloys. Jurak et al. [27] performed experiment in vacuum ultraviolet range (UVU,  $\lambda < 200$  nm) for detection of trace element in polyethylene (PE), at energy 50 mJ and pulse repetition rate of 10 Hz and obtain limit of detection 50  $\mu\text{g/g}$  for sulphur and 215  $\mu\text{g/g}$  for zinc. Schechter et al. [2] reported limit of detection 1  $\mu\text{g/g}$  for the analysis of plant material in the vacuum ultraviolet range (VUV). They reported maximum enhancement at inter-pulse delay at 5  $\mu\text{s}$ , whereas Angel et al. [28] observed maximum signal enhancement at 10  $\mu\text{s}$ . Jiang et al. [29] investigate limit of detection of sulphur and carbon in steel using double pulse LIBS. Hong-Kun et al. [30] studied the quantitative analysis of aluminum alloys at atmospheric pressure, calibration curves of five elements have been extracted and carried out LOD. Lozep-Moreno et al. [31] carried out quantification of elemental composite of low steel alloys using LIBS, calibration curves have been contrasted and LOD is below 100 ppm. Thiem et al. [32] generate plasma using second harmonic in an ultra-high vacuum and LOD was estimated in the range of 20-200  $\mu\text{g/g}$ .

## 1.4 Plasma

Plasma is an ionized gas or other medium in which charged particle interactions are predominantly collected. Plasma is the fourth form of matter that can be obtained when heating a substance to a point where a major fraction of the atoms are separated and form an ionized gas which consists of negatively charged electrons (free electrons) and positive charged ions in addition to neutral atoms and molecules present in the gas. Plasma can be converted from neutral state of matter in many ways, but generally includes absorption of energy from source and generates number of ions and electrons, as whole plasma is neutral.

## 1.5 Laser matter interaction

Laser has its main characteristics such as monochromaticity, directionality, coherence and its intensity which distinguish it from conventional light. Laser emits radiation in continuous form as well as short pulses of duration nanosecond, picosecond and femtosecond. Laser source of irradiance of the order  $10^7 - 10^9 \text{ Wcm}^{-2}$  or greater can be used to generate plasma. When a high intense laser pulse focused on a solid target, plasma is generated by the melting and vaporization of the surface of the target. At the same time, there is no further removal of material from target surface and radiations are absorbed by target surface which results it to expand and increase in its

internal energy. Shock waves produce into the target when expanding layer pressurizes the neighboring layer. Plasma plume has its maximum velocity perpendicular to target surface.

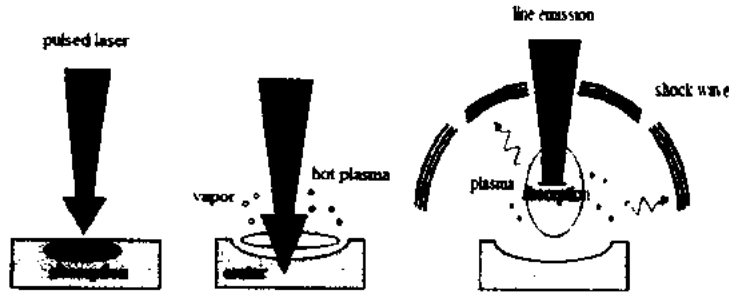


Figure 1.1 Schematic diagram of laser induced plasma

Plasma emits light by following three processes.

Recombination:



De-excitation of ions:



De-excitation of atoms:

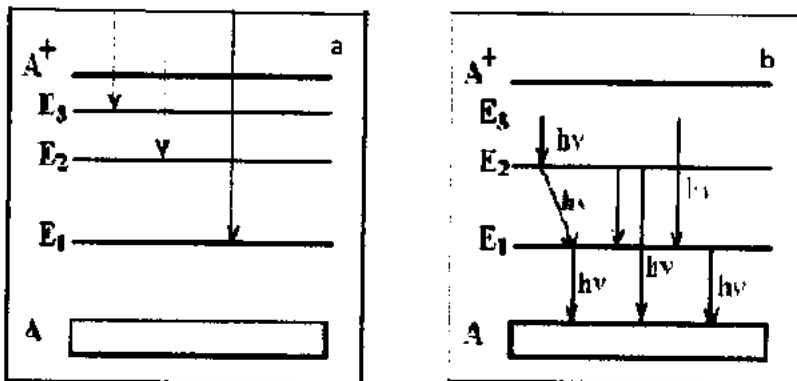
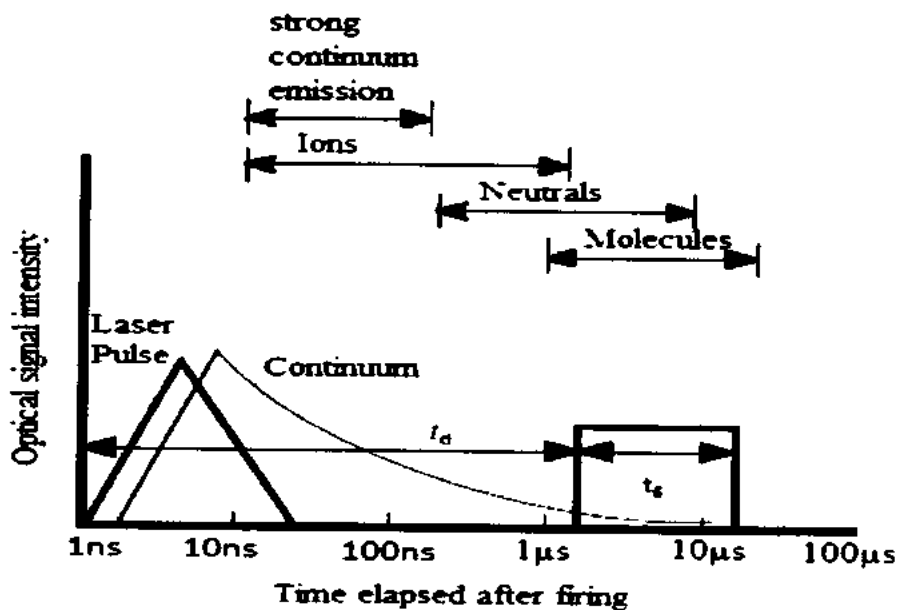


Figure 1.2 (a) shows broadband emission due to bremsstrahlung and free bound transition, (b) shows line emission due to bound-bound transition.

## 1.7 Temporal evolution of LIBS plasma

Time resolution of the plasma light in LIBS allows for discrimination in favor of the region where the signals of interest predominate. Figure 1.3 shows observed spectra at different stages and normal transition in atom and ion. The symbol  $t_a$  represents the delay from the initiation of the laser to the opening of the window during which signals are recorded;  $t_b$  represents the length of time window. LIBS plasma can be produced using double pulse mode, where two laser pulses from the same or different lasers are incident on the target.



*Figure 1.3 A schematic diagram of the temporal history of a LIBS plasma*

LIBS plasma typically weak ionized plasma. Weakly ionized plasma in which ratio of electron to other species is less than 10%. While in highly ionized plasma has high electron to atom / ion ratio. Initially, the ionization is high. Background continuum also present there that decays more quickly. These continuum is basically due to bremsstrahlung and recombination. Where  $E$  is energy in joules, the frequency, wave number and wavelength of transitions is given by  $\nu = \frac{\Delta E}{h}$ . Basically LIBS technique must have to create an optically thin plasma which is in local thermodynamic equilibrium (LTE) and whose elemental composition is the same as that of the sample.

## 1.8 Conventional techniques

Conventional methods for quantitative analysis are inductively coupled plasma mass spectroscopy (ICP-MS), inductively coupled plasma atomic emission spectroscopy (ICP-AES) and x-ray fluorescence. These techniques are still in use but having expensive apparatus, time consuming etc. so that LIBS is preferred over that all.

Inductively coupled plasma mass spectroscopy (ICP-MS) is one of the quantitative analysis technique of metals and non-metals with atomic mass ranges from 7 to 250, it can detect concentration as one part in  $10^{12}$  ppm. By continuous scanning by mass spectrometer, data collected in the form of signal intensities. It is also known as inductively coupled plasma optical emission spectroscopy (ICP-OES). In this technique, inductively coupled plasma is used to detect trace metals present in the sample and excited atoms and ions present in the plasma emit electromagnetic radiation of specific wavelength of particular sample. The intensity of this light shows the concentration of element in the sample. X-ray fluorescence technique is a non-destructive and elemental analysis technique for solid, powder and liquid sample. This technique is used to identify and accurately finds the concentration of element in the sample. This method is used for analysis of rocks and metals with an accuracy of approximately 0.1 % of major element present in the sample. In this technique, high energy x-ray is injected to sample and energy is absorbed by atoms. Electrons from low energy level ejected and outer shell electron fill the orbit and this transition emits x-ray. It is difficult to analyze element lighter than sodium having  $z = 11$ , but beryllium  $z = 4$  also analyzed.

## 1.9 Broadening of spectral lines

In spectroscopic studies, emission of spectral lines in spectrum have definite width rather than sharp line which plays significant role and contains information such that plasma parameters can be determined from it. Line broadening process can be divided into homogeneous and inhomogeneous broadening. Pressure broadening is inhomogeneous and has variation in resonance frequency or line shape for the same transition. All other broadening processes are homogenous in which all atoms have similar transition frequency also resonance line shape. Line shape of spectral lines depends on some broadening process as discussed below.

### 1.9.1 Natural broadening

When electrons are excited to higher energy states, it stays there for some finite time, which is called the life time of that particular state. This life time causes broadening in the line profile, which is termed as a natural broadening. Life time can be measured by using the following uncertainty principle. Here  $\Delta E$  is the energy of the state.

$$\Delta E \Delta t \approx \frac{h}{2\pi} \quad (1.6)$$

And the frequency can be extracted from the life time using following expression.

$$\Delta \nu = \frac{1}{2\pi \Delta t} \quad (1.7)$$

### 1.9.2 Doppler broadening

Doppler's effect occurs due to the relative motion between source and observer. Doppler broadening occurs due to relative motion of the emitted species and results line broadening. This broadening mechanism is prominent in expanding and low density plasma. The Doppler broadened line show best with when fitted with the Gaussian function. The Doppler width can be determined by the following expression [33].

$$\Delta \lambda_D = 7.2 \times 10^{-7} \left( \frac{T}{M} \right)^{1/2} \lambda_0 \quad (1.8)$$

Here the  $M$  is the atomic mass of the element and  $T$  is the temperature.

### 1.9.3 Stark Broadening

Splitting and shifting of energy level as a result of perturbation caused by electric field is known as stark effect. Stark broadening is a special case of pressure broadening in which interaction of atoms with charged particles such as ions and electrons, will slightly changes the energy levels leading to broadening of spectral lines. The magnitude of perturbing electric field ( $F$ ) created by slow moving ions and fast moving electrons at a certain distance is given by

$$F = \frac{1}{4\pi\epsilon_0} \frac{e^2}{r^2} \quad (1.9)$$

Stark effect is dependent on field strength, is either linear or quadratic. Linear stark effect (F), is only for hydrogen atom where splitting is proportional to electric field strength F. Linear stark effect shifts the energy level symmetrically broaden but un-shifted line. Stark broadening of isolated lines used to calculate electron number density.

### 1.10 Determination of electron number density

The number of free electrons per unit volume known as electron density or plasma density. The electron number density ( $N_e$ ) can be calculated from stark broadening and it is the main parameter for showing plasma induced by the laser. Other mechanisms which are Doppler broadening and natural broadening also takes place when in a low density and high temperature plasma. The FWHM  $\Delta\lambda_{1/2}$  of a Stark broadened line is given as [34].

$$\Delta\lambda_{1/2} = 2\omega \left( \frac{N_e}{10^{16}} \right) + 3.5A \left( \frac{N_e}{10^{16}} \right)^{1/4} \left[ 1 - \frac{3}{4} N_D^{-1/3} \right] \omega \left( \frac{N_e}{10^{16}} \right) \quad (1.10)$$

Here,  $N_e$  ( $\text{cm}^{-3}$ ) is the electron number density,  $A$  (nm) is the ion broadening contribution,  $\omega$  (nm) is the electron impact parameter and the number of particles in a Debye sphere is represented by  $N_D$ . The following expression determines the  $N_D$  the Debye sphere [35].

$$N_D = 1.72 \times 10^9 \frac{T^{3/2}}{N_e^{1/2}} \quad (1.11)$$

The first part of Eq. (1.10) represents the broadening due to electrons, whereas the part is ionic contribution in line broadening. The ions are heavier, therefore their contributions is negligibly small and the approximate expression is as follows,

$$\Delta\lambda_{1/2} = 2\omega \left( \frac{N_e}{10^{16}} \right) \quad (1.12)$$

The number  $10^{16}$  in the denominator of above equation has the unit of  $\text{cm}^{-3}$  to make it dimensionally correct.

### 1.11 Determination of plasma temperature

The electron temperature of laser induced plasma is the fundamental parameters for the understanding and characterization of laser induced plasma. The method of electron temperature determination is described below.



### 1.11.1 Boltzmann plot technique

For the determination of electron temperature, Boltzmann plot technique is mostly used because of improved accuracy. This method uses multiple emission lines for the estimation of electron temperature. The population distribution between two energy levels is as follows [33].

$$\ln\left(\frac{\lambda_{pi} I_{pi}}{hc A_{pi} g_p}\right) = \ln\left(\frac{N(T)}{Z}\right) - \frac{E_p}{kT} \quad (1.13)$$

The plot of left side of Eq. (1.13) as a function of upper state energy  $E_p$  gives linear fit with slope  $-\frac{1}{kT}$ , which yield electron temperature. For reliable temperature, the spectroscopic data should be accurate and well-spaced transition should be used.

### 1.11.2 Plasma temperature using Intensity Ratio method

Plasma temperature can be calculated from intensity ratio method in which ratio of intensities of intensities of spectral lines of same ionization level of the same element. The relative intensity of transition lines whose de-excited state is same, can be given as,

$$\frac{I_1}{I_2} = \frac{g_1 A_{1\lambda_1}}{g_2 A_{2\lambda_2}} \exp\left[-\left(\frac{E_2 - E_1}{KT_0}\right)\right] \quad (1.14)$$

Where subscripts 1, 2 are used two spectral lines of same element and I, g,  $\lambda$ , A, E are line intensities, statistical weight, wavelength, transition probability and energy of excited state.

## 1.12 Local thermal equilibrium (LTE)

Methods for determination of electron temperature as discussed are applicable when the plasma is in local thermal equilibrium (LTE) i.e. the collisions must be dominant over radiative processes. In other words, in excited state, de-excitation through collisions must be higher as compare to spontaneous emissions. This condition must be applicable to get high electron number density to attain LTE. Detailed analysis is available in "Laser induced breakdown spectroscopy" [2]. The following Mc Whirter's relation is used for LTE to fulfill [36].

$$N_e \geq N_{cr}$$

$$N_e \geq 1.6 \times 10^{12} T^{1/2} (\Delta E)^3 \text{ cm}^{-3} \quad (1.15)$$

Where,  $N_e$  is the measured number density,  $\Delta E$  (eV) is the transition energy and  $T_e$  (K) is the electron temperature.

### 1.13 Plasma opacity and self-absorption

When the radiation emitted does not reabsorbed, the plasma is optically thin and the phenomenon is called plasma opacity. The emission intensities are used to infer whether the plasma is thick or thin. The plasma is optically thin after the intensities follow the intensity selection rules. But, if the line intensity deviating and plasma density is high, plasma reabsorb the emitted light, and intense emission lines saturated or flat-topped profile, the plasma is optically thick. In addition to self-absorption, there may be a dip at center of emission line, which is known as self-reversal due to the reason that emitted photons passes through the cold part of the plume.

### 1.14 Quantitative analysis using calibration curve

For both qualitative and quantitative analysis, main requirement is emission spectra. Main methods for quantitative analysis are calibration and calibration free methods are explained.

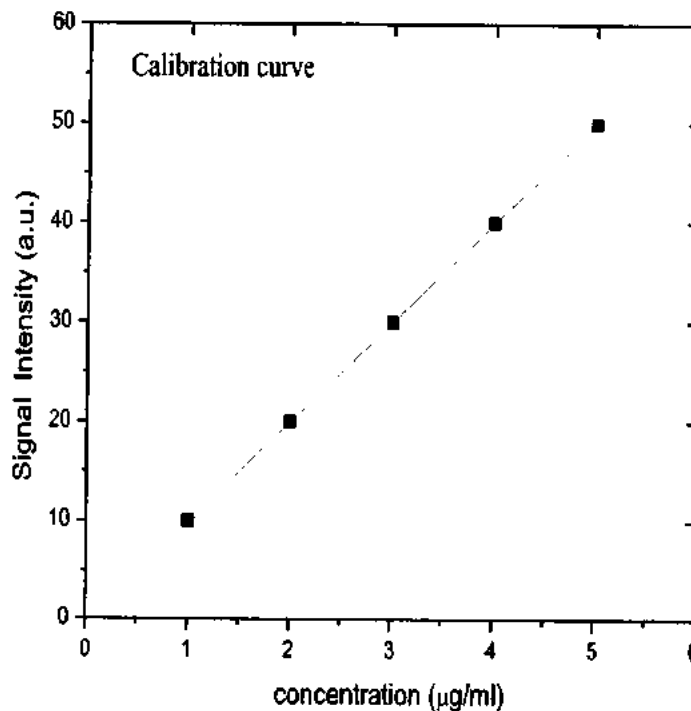


*Figure 1.4 Calibration curve concentration vs signal intensity*

In LIBS, calibration curve is the most common method. Calibration curve is constructed between intensity and concentration (%). In this method, standard sample having known concentration of element is added and in this way we can find concentration of an unknown sample by fitting emission intensity on standard calibration curve. Firstly, the emission spectra of standard samples are taken and are analyzed and graph is constructed between emission intensity and concentration. Secondly, take the emission spectra of unknown sample, by comparing the intensity of this unknown sample, we can estimate the concentration of unknown sample. To detect the trace element in the sample in parts per million (ppm), calibration curve is constructed between LIBS signal intensity and concentration of element present in different sample as shown in figure 1.4.

### 1.15 Limit of detection

The limit of detection (LOD) is the smallest amount of the analyte that can be detected and be determined experimentally. It is usually expressed as the minimum concentration,  $C_L$  or the quantity,  $q_L$ , which can be detected with good accuracy.

$$X_L = X_{bi} + ks_{bi} \quad (1.16)$$

Here  $X_{bi}$  is the mean of blank measure,  $s_{bi}$  is the standard deviation of the blank measure and  $k$  is a constant related to the confidence level. The slope of the calibration curve is given by  $m = \frac{\Delta X_L}{\Delta C_L}$ ,  $C_{bi}$  is usually zero that tell us that no analytic concentration in the blank sample. Limit of detection can be found by using relation

$$C_L = \frac{ks_{bi}}{m} \quad (1.17)$$

Ideally, using  $k = 3$  for determination of LOD. This value will give correspond to a confidence level of 90,  $m$  bc the slop of calibration curve. In this experiment we are interested for quantitative analysis of silver in polymer.

The limit of detection (LOD) is the term used to describe the smallest concentration that can be measured with sufficient accuracy. The requirement, importance and application of the knowledge of LOD is useful in each area, where reliable measurements are critical. In analytical measurements, such as LIBS, first we have to decide, whether the particular specie is present or not. To decide reliable, we have to measure the LOD, which makes LOD the basis of all the analytical measurements. Moreover, the evaluation of LOD is necessary because some elements

are harmful and dangerous for health as reported by Godwal et al. [37] and their detection and quantification is very much necessary.

## 1.16 Polymer and sample description

Word polymer is Greek word in which 'polus' mean 'many' and 'meros' mean 'parts'. Polymer is a large molecule or macro molecule composed of many repeated units in three dimension. Polymer are of two types, both types of polymers are formed through polymerization of many small molecules called monomers.

- Natural polymer which includes wool, silk and rubber.
- Synthetic polymer includes synthetic rubber, polyvinyl chloride (PVC), polystyrene, polyethylene, polypropylene, polymethyl methacrylate (PMMA) and many more.

### Polymethyl methacrylate (PMMA)

In the present work, thin film of commonly available polymer polymethyl methacrylate (PMMA) are prepared using the known concentration of silver nitrate ( $\text{AgNO}_3$ ). Sample preparation is describe in chapter 2. Mostly it is called acrylic glass or simply acrylic and it is in crystalline form. The chemical formula of PMMA is  $(\text{C}_5\text{O}_2\text{H}_8)_n$  and molecular mass 100 g/mol. Its melting point is  $130^\circ\text{C}$ . Solvent for PMMA is acetone which is colorless liquid its chemical formula is  $\text{C}_3\text{H}_6\text{O}$  and its melting point is  $-95.35^\circ\text{C}$ .

### Silver nitrate ( $\text{AgNO}_3$ )

Its chemical formula is  $\text{AgNO}_3$  and molecular mass 169.87 g/mole, having orthorhombic structure. Its melting point is  $209.7^\circ\text{C}$  and is odorless. Solvent for silver nitrate is ethanol. Its chemical formula is  $\text{C}_2\text{H}_6\text{O}$  and its melting point is  $-114^\circ\text{C}$

## 1.17 Double pulse LIBS

Main limitation of LIBS is its low sensitivity, to overcome this, double pulse with different configuration are used to enhance signal intensity and signal to noise ratio. Different configuration involve collinear, orthogonal, cross orthogonal are mainly used. We in our practical collinear is used as it is simple and easy configuration.

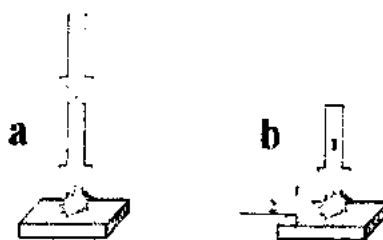


*Figure 1.5 Schematic representation of different double –pulse configuration (a) shows collinear, (b) orthogonal reheating*

In collinear configuration, two laser pulses, with inter pulse delay from picosecond to microsecond to generate plasma. Two pulses propagate in the same direction and both directed to target. First laser produce plasma and second laser reached with some inter-pulse delay, reheating the plasma produced by first laser. Plasma changes in rectified gas air enclosed by shock wave created by the first laser pulse. In orthogonal configuration, first laser move parallel hits the target and generate plasma on the surface and second pulse propagate orthogonal to target. Double pulse gives flexibility in wavelength, pulse width and pulse sequence. Experimentally, collinear double pulse is easy for double pulse LIBS.

## 1.18 LIBS Applications

LIBS is a simple technique having little or no sample preparation. It can be used for real time analysis. Some major advantages of LIBS technique make it more valuable. The study of soils and minerals which are useful in mining and geology.

1. Analysis of planets to recognize the elemental structure of Mars and Venus etc.
2. Analysis of hair tissues, cancer and teeth, and DNA types of study.
3. Detection of explosives for security reasons in defense system.
4. Checking the quality of metals and alloys in metallic industry.
5. Detection of radioactive elements in nuclear industry.
6. LIBS has capability to determine elemental composition of different materials, whether the sample may be solid, liquid gas or aerosol.
7. LIBS is also used for remote analysis.

### Experimental Setup and Procedure

This chapter represents a brief description of the experimental setup and the instrumentation used in our experimental setup. The description of the instrumentation includes laser system, sample preparation, beam delivery and data collection and analysis. The experimental procedure for the plasma generation using single and double pulse is described in this chapter.

#### 2.1 Sample preparation

The reference samples of polymers of known concentration of silver were prepared by solvent casting method. The silver nitrate solution was prepared by mixing 10 mg silver nitrate to 10 ml ethanol and stirrer it for approximately 30 minutes as shown in figure 2.1. This stock solution say A of which 1 ml having 1 mg of  $\text{AgNO}_3$  say B is mixed with 1 ml ethanol and thus made serial dilutions by adding 1 ml ethanol each time. In this way, we made solution with concentration of  $\text{AgNO}_3$  up to  $0.24 \mu\text{g}$ .



*Figure 2.1 Magnetic stirrer used for solution mixing*

In the next step, we made a solution of PMMA by adding acetone in it and the solution of  $\text{AgNO}_3$  have been doped in as follows. We took 3 ml acetone and 0.94 g of PMMA in a beaker and put it in magnetic stirrer hotplate for 2-3 hours. Similarly five more solutions of 3 ml acetone and 0.94 g PMMA separately. Finally, 3 ml of acetone was mixed with PMMA solution to the silver nitrate solution and placed on magnetic stirrer hotplate for 20 minutes. The mixed solution was put into individual patri dish and placed these patri dishes into a leveled place for 16-20 hours

## Experimental Setup and Procedure

---

(Solvent Casting Method). The acetone and ethanol got evaporated and 40  $\mu\text{m}$  thin films prepared as shown in figures 2.2 and 2.3. Figure 2.2 shows blank sample (without doping) having 2 " diameter and 40  $\mu\text{m}$  thickness, whereas doped samples of different concentration of  $\text{AgNO}_3$  are shown in Figure 2.3.

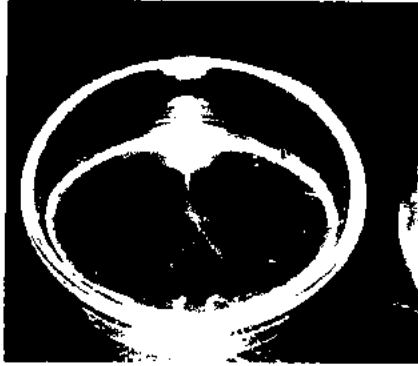


*Figure 2.2 Blank sample of PMMA in patri dish*

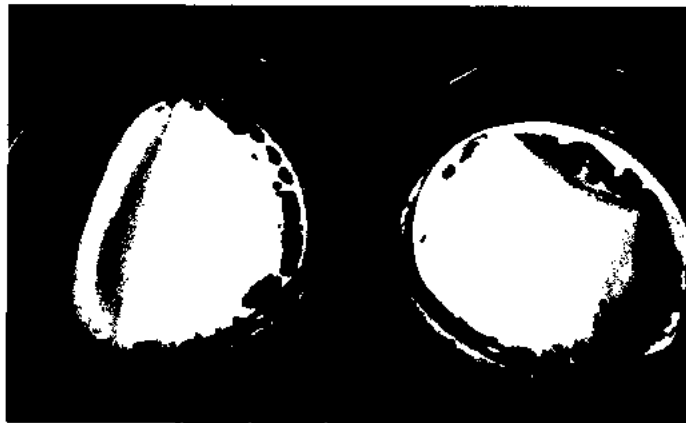


*Figure 2.3 Thin film sample of PMMA doped with different concentration of  $\text{AgNO}_3$*

### 2.2 LIBS Instrumentation

In LIBS, the intense beam is shine on sample to generate plasma. The plasma arc collected and directed on the detector through optical fiber. In the present experiment, LIBS setup consists of three main parts,

- i. Nd: YAG laser system for plasma generation,
- ii. LIBS 2500+ spectrometer fitted with charged coupled device,
- iii. Sample chamber.

## Experimental Setup and Procedure

### 2.2.1 Laser system

Laser is used to generate plasma plume on the sample surface. A variety of laser systems are used for this purpose ranging from IR to UV and from nanosecond to femtosecond. Commonly used laser system includes Excimer lasers XeCl (308 nm), KrF (248 nm), ArF (194 nm), CO<sub>2</sub> laser (10.6 μm), ruby laser (693 nm), Nd: YAG laser (1064 nm, 532 nm, 355 nm) and femtosecond laser system. Among these lasers Nd: YAG laser is widely used in LIBS experiment due to easy handling and operating.

#### Nd: YAG laser

Nd: YAG laser system, Yttrium Aluminum Garnet (Y<sub>3</sub>Al<sub>5</sub>O<sub>12</sub>) crystal is used as host medium in which 1% of Y<sup>+3</sup>, are replaced by Nd<sup>+3</sup> (triple ionized neodymium) ions which serves as an active medium. Nd: YAG laser system is a four level system in which pump source is flash lamp. The Nd: YAG laser operates at 1064 nm as a fundamental wavelength, whereas 532 nm and 355 nm wavelengths can be obtained as a 2<sup>nd</sup> and 3<sup>rd</sup> harmonics. These harmonics are produced by using nonlinear crystals. These are two main pump bands at 730 nm and 800 nm which are coupled by a fast non-radiative decay to the <sup>4</sup>F<sub>3/2</sub> level from where decay to the lower level <sup>4</sup>I<sub>11/2</sub> as shown in figure 2.4. The rate of decay is much slower (t = 0.23 ms), but this transition is prohibited permitting to electric dipole transition rules ( $\Delta J = 0, \pm 1, 0 \neq 0$ ), however becomes weakly allowed due to crystal field interaction. The transition from <sup>4</sup>F<sub>3/2</sub> to <sup>4</sup>I<sub>11/2</sub> is the most strong and intense transition out of various possible transitions from <sup>4</sup>F<sub>3/2</sub> to lower levels. The <sup>4</sup>I<sub>11/2</sub> level has short life time and atoms quickly decay non- radiative to the <sup>4</sup>I<sub>9/2</sub> ground level.

In the present work, we have used two Nd: YAG Lasers (Brilliant B, Quantel). The specifications of these systems are listed in table 2.1.

*Table 2.1 Specifications of Nd: YAG laser*

	1064 nm	532 nm	355 nm
	8.5 W	4W	1.85 W
	850 mJ	400 mJ	185 mJ
	6 ns	5 ns	5 ns
		< 0.5mrad	
		1.0 cm <sup>-1</sup> at 1064 nm	



## Experimental Setup and Procedure

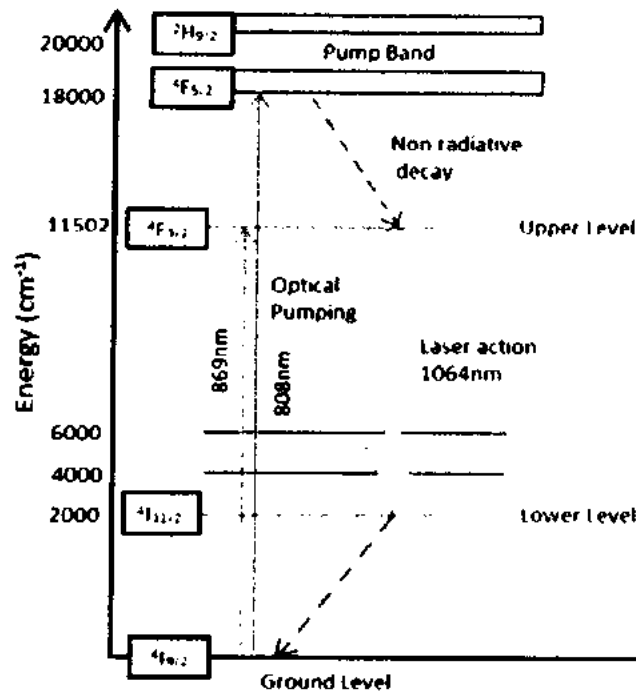


*Figure 2.4 Energy level diagram of the trivalent neodymium ion.*

### Nature of Gaussian Beam

The laser beam used in the present work is of Gaussian nature, but in order to confirm its Gaussian nature we recorded laser beam profile.

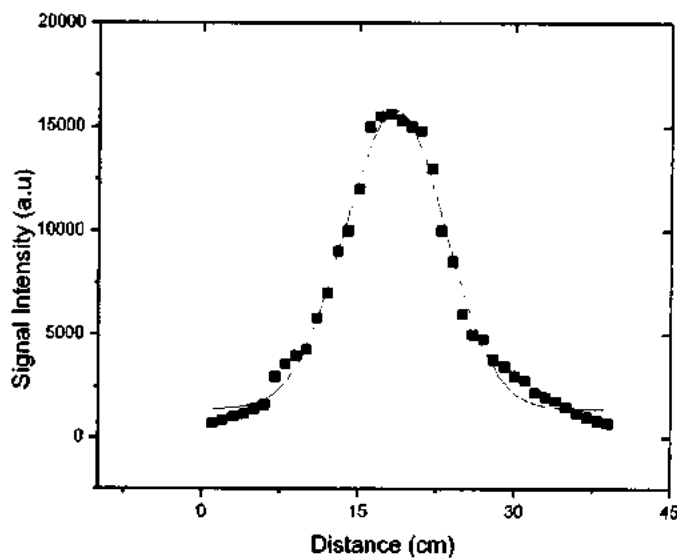


*Figure 2.5 Laser beam profile, showing an intensity profile*

## Experimental Setup and Procedure

The 2<sup>nd</sup> harmonic (532 nm) from the Nd: YAG laser is shine on a diverging lens and get expanded laser beam. We fixed the optical fiber probe of HR4000 spectrometer on a sliding stage and placed this assembly in front of the expanded laser beam. The fiber probe was moved in small steps across the laser beam and signal intensity was recorded. The recorded signal intensity was plotted as a function of distance across the beam as shown in Fig.2.5. The best fit over these data points was the Gaussian function, which confirmed that the laser beam is of Gaussian nature.

### 2.2.3 Beam focusing and collection system

The beam focusing part of the setup consists of beam delivery and focusing laser beam on the target surface. Mirrors were used to direct laser beam on the target and focusing lens focused the laser beam. Focusing is necessary in order to achieve the minimum laser irradiance required for plasma generation. The focusing arrangement is shown in Fig. 2.6. The emissions associated with plasma is collected via collection lens and directed on the fiber, which transmitted this light to the spectrometer. Spectrometer received the light, dispersed it and displayed in a readable format.

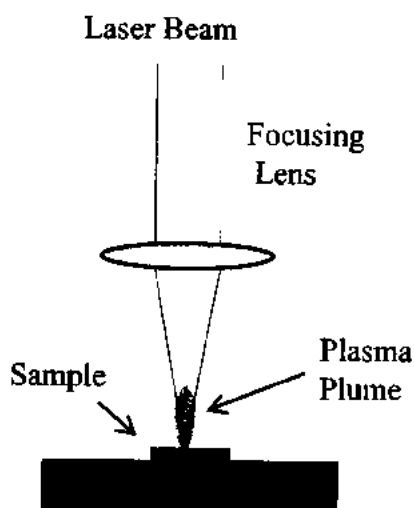


*Figure 2.6 Formation of plasma plume*

### 2.2.4 Sample stage

Sample stage consists of rotating stage placed inside sample chamber. The rotating sample holder is used place thin film sample on it and the laser shots hits the fresh surface each time. The sample was placed in such way that laser beam falls on it vertically. Fig. 2.7 shows the photographic view of the chamber used in the present work. In addition to sample sitting arrangements, this chamber has fiber holder, which is located near the sample surface and is used for plasma light collection



*Figure 2.7 Sample placed inside the sample chamber*

### **2.2.5 LIBS-Spectrometer**

In the present work, we have used seven channel LIBS 2500+ spectrometer from ocean optics. Each channel has one small HR2000 spectrometer, which are lumped together in one assembly as shown in Fig. 2.8. This spectrometer is designed for LIBS experiments having spectral range from 200-980 nm and resolution of 0.1 nm. Spectrometer is connected to PC through USB port. The OOILIBS software is used to control the laser firing and recording the emission spectra.

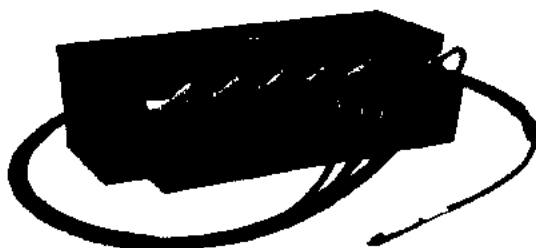


*Figure 2.8 Seven channel LIBS 2500+ spectrometer*

### **HR 2000 Spectrometer**

The light emitted from plasma enters through slit and falls on collimating mirror which transmits it to grating. Light falls on another mirror on different wavelength. After reflecting through this mirror, light falls on CCD detector which converts light into digital signal and we collect its output through OOI LIBS software. All the components are built together in one housing as shown in Fig. 2.9. The component wise detail is as follows:

## Experimental Setup and Procedure

---

- **SMA Connector**

Emission produced by plasma plume enters the optical bench through SMA connector. It is labeled in figure 2.9.

- **Slit**

It is rectangular aperture, mounted on the back of SMA connector. This part is the entrance of light to spectrometer. It control the amount of light entering the spectrometer and its width is linked with spectrometer resolution.

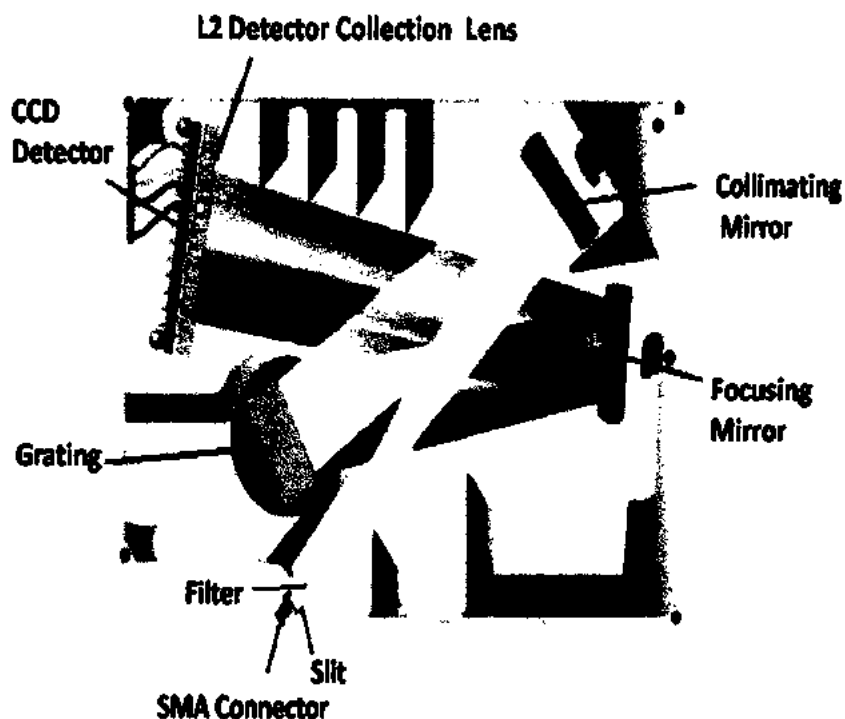


*Figure 2.9 LIBS spectrometer with components.*

- **Filter**

Filters are used to limit the emission to a specific wavelength, before it enters into optical bench. Band pass and long pass filters are used to limit the emission.

- **Collimating Mirror**

After passing through filters, light falls on broadband collimating mirror that diffract light to grating.

## Experimental Setup and Procedure

---

- **Grating**

Grating is one of the key component of a spectrometer. The Purpose of the grating in spectrometer is to diffract light onto the focusing mirror. Gratings allow specific wavelength selection and its resolution depends on the wavelength range. Light from grating dispersed on focusing mirror.

- **Focusing Mirror**

Light from grating directs on focusing mirror and is detected by CCD detector.

- **Detector collection lens**

Detector collection lens having large diameter slits is used to focus light onto the CCD detector elements, which is received from focusing mirror.

- **CCD Detector**

It is the most imported component of the spectrometer which convert electronic signal into digital signal which is then send to OOI LIBS software through which we collect spectrum.

### Working of CCD

Charged coupled device (CCD) is silicon substrate, divided into number of small sections. Each section is known as pixel (potential well) as in figure 2.10. Photons of light when falls on these pixels, it converted into electrons and collected in potential well. In this way, more and more electrons are collecting in potential well. A point reached when no further electron will be collecting in potential well, this point is known as saturation. To avoid saturating condition, shutter is used.

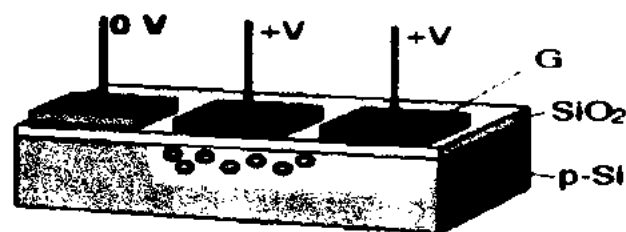


*Figure 2.10 shows silicon based Charged Couple Device (CCD) consists of pixels which converts photons of light into electrons.*

## Experimental Setup and Procedure

Each pixel consists of three electrodes, one of which is at high potential create potential well and the other two electrodes (low potential) transfer charges out of CCD. In this way charges will be clocking out either by down the column or across the row, depending on the orientation of electrodes as shown in figure 2.11. Resolution of CCD depends on size of pixel i-e, number of rows and number of columns and pixel pitch.

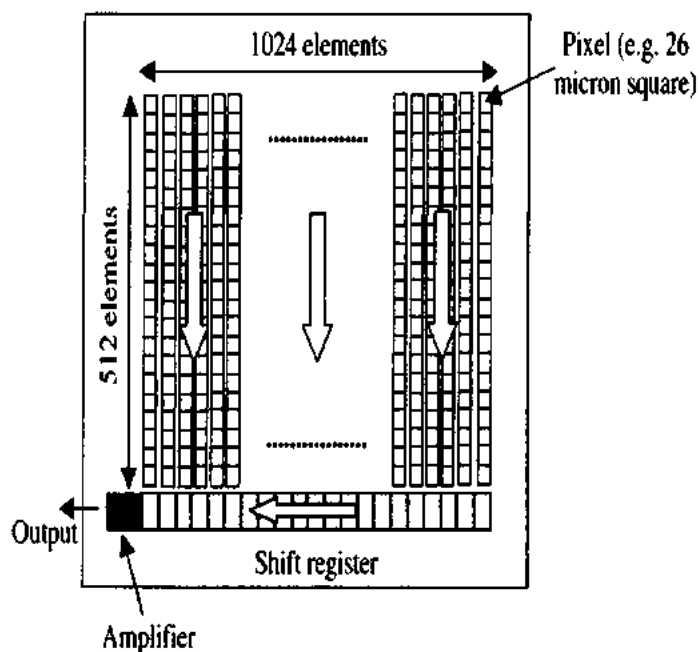


*Figure 2.11 Clocking out of charges row wise.*

### 2.2.6 LIBS software

Emissions from plasma are collected through fiber from detector and spectrum can be taken using OOI LIBS software in the display screen of computer, installed windows XP.

### 2.2.7 Spectral Resolution

One of the main features of spectrometer is its spectral resolution. Spectral resolution resolves the minimum spaced peaks. It depends on slit, grating and CCD. Slit defines minimum image size that the optical bench can form in the detector level. The diffraction grating limits the total wavelength range of spectrometer. The detector defines the maximum number and size of understated points in which spectrum can be digitized. Spectral resolution of spectrometer that we use in our experiment is 0.1 nm, having range 200-980 nm.

## Experimental Setup and Procedure

### 2.3 Experimental Procedure

The experimental setup for the determination of limit of detection and estimation of plasma parameters is shown in figure 2.12.

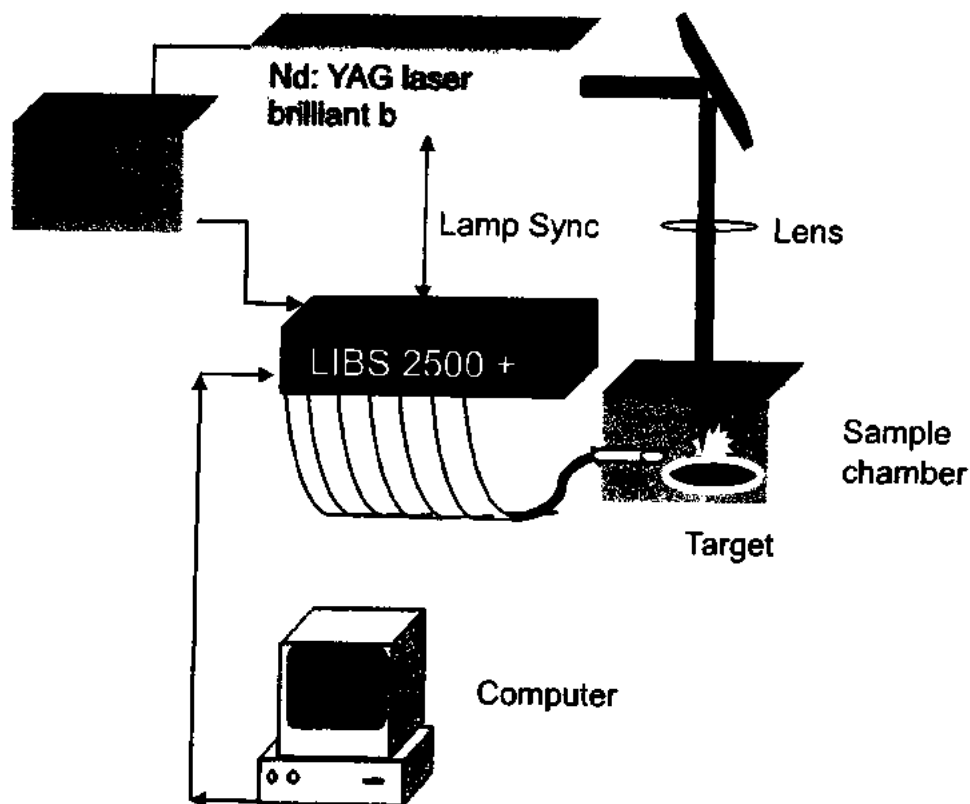


*Figure 2.12 Experimental setup of LIBS.*

We used Q-switched Nd: YAG laser (Quantel Brilliant b) having pulse duration 6 ns, rep. rate per pulse 10 hertz and capable of delivering 850 mJ at 1064 nm, 400 mJ at 532 nm and 185 mJ at 355 nm. The energy of laser pulse was controlled from the remote control of laser by varying Q-switch Flash-Lamp delay and was monitored by energy meter (TOP MAX III, Coherent, USA). The laser pulse was focused on the sample through lens of 5 cm focal length. The already prepared thin film samples in circular shape of diameter 2" and thickness 40  $\mu\text{m}$  have been placed on rotating stage to provide fresh surface every time to laser pulse. The focused laser beam thus produced plasma on its surface and the plasma emissions were collected by an optical fiber with collimating lens 0-45 degrees field of view. The fiber was placed at right angle to the direction of laser beam and its output was coupled to 10  $\mu\text{m}$  wide entrance slit of LIBS 2500+ spectrometer (Ocean Optics, USA). The LIBS 2500+ system, equipped with seven spectrometers covering the range between

## Experimental Setup and Procedure

200-980 nm having resolution of 0.1 nm and 2.1 ms integration time. To get better signal-to-noise ratio, the gate delay was set 2  $\mu$ sec after laser firing. The output signal of the CCD was processed and analyzed using OOI LIBS software and displayed in the form of a spectrum. The LIBS system triggered the Q-switch of Nd: YAG laser and were synchronized through lamp synchronization.

Each spectrum was recorded using a single laser shot and such ten data sets were averaged to overcome the fluctuations in the spectra. The recorded spectra were analyzed using wavelength and energy data of NIST database. The emission lines were assigned and confirmed by comparing the observed intensity ratio to that reported in NIST database. We have also considered the transition probabilities in assigning the emission lines

Since double technique enhances the signal intensity and improve the limit of detection, therefore, in the present work this configuration has been applied. According to the schematic diagram in Fig. 2.13, the laser pulses from two lasers with variable delay were used in collinear configuration. An Nd: YAG, laser (Brilliant B, Quantel) operating at its fundamental wavelength of 1064 nm was used as a first laser to ablate the sample, whereas the second pulse of the same wavelength from Nd: YAG laser (Brilliant B, Quantel) was irradiated which reheat the plasma.

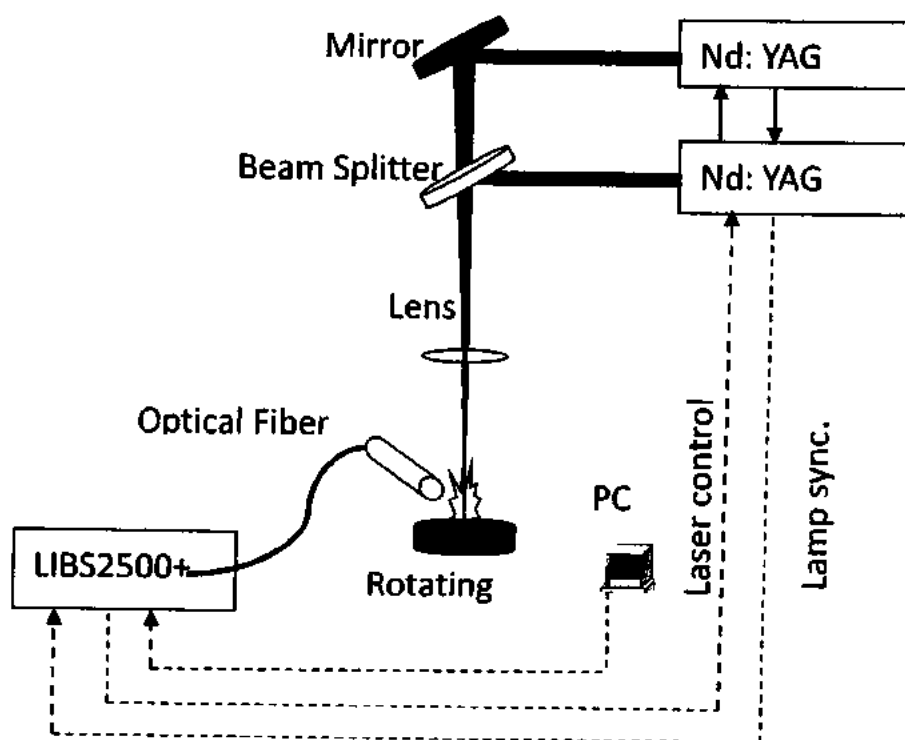


**Figure 2.13** Collinear double pulse LIBS setup



## Experimental Setup and Procedure

---

Both the lasers were synchronized using flash lamp synchronization and delay between pulses was adjusted using delay generators. In double pulse LIBS, the inter-pulse delay and ratio of laser energy pulses has important role in signal enhancement, sensitivity and improvement in limit of detection. In the present work, the inter pulse delay and the energy ratio of the first and second laser were optimized to get better signal to noise ratio. The signal intensity of 308.24 nm, 358.7 nm and 393.4 nm emission lines were plotted as a function of inter-pulse delay and energy ratio. The plot yield that signal is higher at 5  $\mu$ s inter-pulse delay and 60/60 mJ energy ratio. These optimized parameters have been used and the mission spectra have been recorded. The detection system triggered the Q-switch of first laser and the Q-switch out of this laser was used to trigger the delay generator (SRS, DG 535), which subsequently triggered the Q-switch of second laser. The delay generator was used to insert delay between two laser pulses. The flash lamps of both the lasers and the detection system were synchronized to each other.

### Experimental Results and Discussion

#### 3.1 Emission spectra of Silver Nitrate doped Polymer

The emission spectra of silver nitrate doped polymer have been recorded for the detection of trace element present in polymer. The plasma of polymer has been produced at atmospheric pressure using 1064 nm wavelength of Nd: YAG laser in a single and double pulse mode. Fig.3.1 shows portion of the emission spectra acquired using single pulse at 120 mJ energy. This spectrum was recorded at a time delay of 2 microseconds with respect to laser pulse to avoid strong background emissions present in the early stage plasma. This later stage plasma emissions show a dominating features of atomic emission lines in a good signal to noise ratio. The spectrum covers the spectral range from 320 to 600 nm, having number of neutral and singly ionized emission lines of silver. A number of spectral lines of calcium (Ca), sodium (Na), and molecular bands CN and C<sub>2</sub> swan bands are also detected with fairly good emission intensity. The transitions are assigned according to LS coupling selection rules ( $\Delta l = \pm 1$ ,  $\Delta J = 0, \pm 1$  where  $J = 0 \leftrightarrow 0$  is not allowed), and NIST atomic spectral database. As shown in figure 3.2 and 3.3 respectively, the emission lines at 328.06 nm, 338.28 nm, 521.91 nm and 546.55 nm identified and designated as the  $4d^{10} 5p^2 P_{3/2} \rightarrow 4d^{10} 5s^2 S_{1/2}$ ,  $4d^{10} 5p^2 P_{1/2} \rightarrow 4d^{10} 5p^2 S_{1/2}$ ,  $4d^{10} 5d^2 D_{3/2} \rightarrow 4d^{10} 5p^2 P_{1/2}$ , and the  $4d^{10} 5d^2 D_{5/2} \rightarrow 4d^{10} 5p^2 P_{3/2}$  transitions of silver. The line at 422.6 nm is assigned as  $3p^6 4s 4p^1 P_1 \rightarrow 3p^6 4s^2 {}^1S_0$  transition of neutral calcium, whereas at 393.3 nm and 396.8 nm a singly ionized lines of calcium are detected and assigned as  $3p^6 4p^2 P_{3/2} \rightarrow 3p^6 4s^2 S_{1/2}$  and  $3p^6 4p^2 P_{1/2} \rightarrow 3p^6 4s^2 S_{1/2}$  transitions.

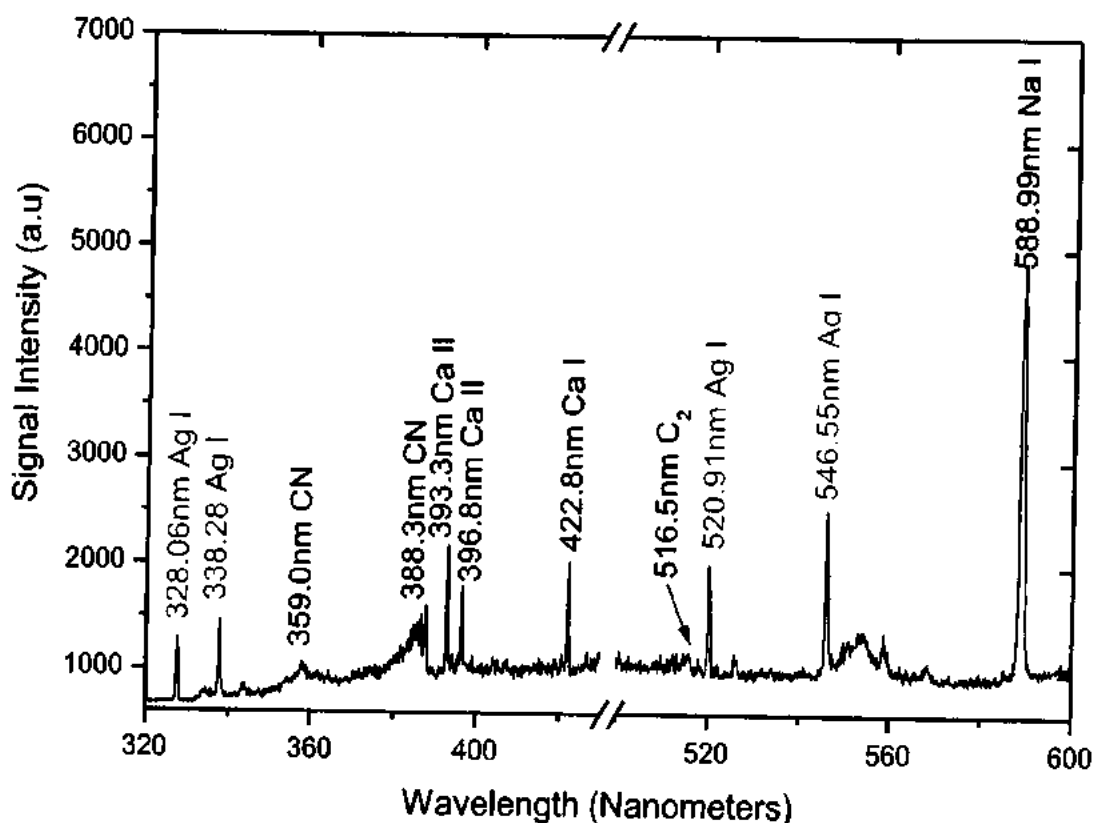


*Figure 3.1* Portion of emission spectrum of silver nitrate doped polymer using single pulse LIBS at 120 mJ per pulse energy. The emission lines of Ag, Na, Ca, CN and C<sub>2</sub> are evident in the spectrum.

An intense emission line at 588.99 nm is assigned as  $2p^6 3p \rightarrow 2p^6 3s$  transition of sodium. The emission lines of silver and calcium are evident in figure 3.2 and 3.3. The molecular bands CN and C<sub>2</sub> are also detected in the spectra of polymer. The CN Violet band at 359.0 nm and 388.3 nm is assigned as  $B^3 \Sigma^+ \rightarrow X^2 \Sigma^+$ . At 516.5 nm C<sub>2</sub> swan band are assigned as  $(D^3 \Pi_g \rightarrow a^3 \Pi_u)$ . The dominant emission lines of silver, appeared in the spectra are due to the doping of silver nitrate in polymer. Whereas the elements like calcium (Ca), sodium (Na), CN and C<sub>2</sub> molecular bands belong to the polymer.

## Experimental Results and Discussion

---

emission lines of sodium, calcium together with molecular bands ( $C_2$  swan band and CN violet band) Sattmann et al. [39] worked out polymer emission spectra in the UV and visible region and used for the identification of different polymers like high-density polyethylene (HDPE), low density polyethylene (LDPE), polyvinyl chloride (PVC), polyethylene terephthalate (PET), and polypropylene (PP). Jurak et al. [27] used  $F_2$  laser ( $\lambda = 157$  nm) having 20 ns laser pulse width, 50 mJ pulse energy and 10 Hz repetition rate for plasma generation on the surface of polyethylene (PE). They extracted the limit of detection (LOD) 50  $\mu\text{g/g}$  and 215  $\mu\text{g/g}$  for sulphur and zinc respectively.

The spectra recorded in the present work are in good agreement to earlier work with respect to element identification and the presence of CN and  $C_2$  molecular bands. We have used these analyzed spectra for the building of calibration curves, for finding limit of detection and for the measurement of plasma parameters. In this work, we have to study the effects of double pulse LIBS on the emission intensities, calibration curves and particularly on the limit of detection. Therefore, we apply double pulse LIBS in collinear configuration and recorded the emission spectra as described in the following section.

### 3.1.1 Double pulse LIBS

In order to have more enhanced emission spectra of the silver nitrate doped polymer, we applied double pulse laser induced breakdown spectroscopy. The aim of this study was to detect the emission lines of silver which are present as a trace or ultra-trace and to investigate the improvement in the limit of detection (LOD) due to double pulse LIBS. It is well known that elemental concentration is directly proportional to the emission intensity of the lines of that element. Therefore, in order to compare with single pulse data, sample of same concentration was atomized. In double pulse arrangement, two delayed laser pulses from two lasers were used in collinear configuration. Nd: YAG, laser (Brilliant B, Quantel) operating at its fundamental wavelength of 1064 nm was used as a first laser to ablate the sample, whereas the second pulse of the same wavelength from another Nd: YAG laser (Brilliant B, Quantel) was irradiated on the plasma which reheat the plasma. The inter pulse delay and energy ratio of the laser pulses have important role in signal enhancement, sensitivity and improvement in limit of detection. The optimization of inert pulse delay and energy ration is described below.

## Experimental Results and Discussion

### Effect of Inter-Pulse Delay

As mentioned earlier, the delay between two laser pulses significantly affect the signal intensity in terms laser matter interaction and plasma coupling. In the present work, the inter pulse delay was increases up to 10  $\mu\text{s}$  and the emission spectrum has been acquired. The signal intensities of 308.24 nm, 358.7 nm, 393.4 nm emission lines have been plotted as a function of inter pulse delay. Figure 3.4 show that initially the signal intensity is low, which increased to maximum at 5 microseconds inters pulse delay and thereafter a decrease is observed up to 10 microseconds. The maximum enhancement in signal intensity at 5 microseconds inter pulse delay show that at this delay the coupling of laser light with target material and with the plasma produced by the first laser is optimum. The variation of signal intensity with inter pulse delay has also been reported by Rizwan and Baig [40] as an optimization step in double pulse experiments. They reported maximum enhancement at 5 $\mu\text{s}$  inter-pulse delay, whereas Angel et al. [41] observed maximum signal enhancement at 10  $\mu\text{s}$ .

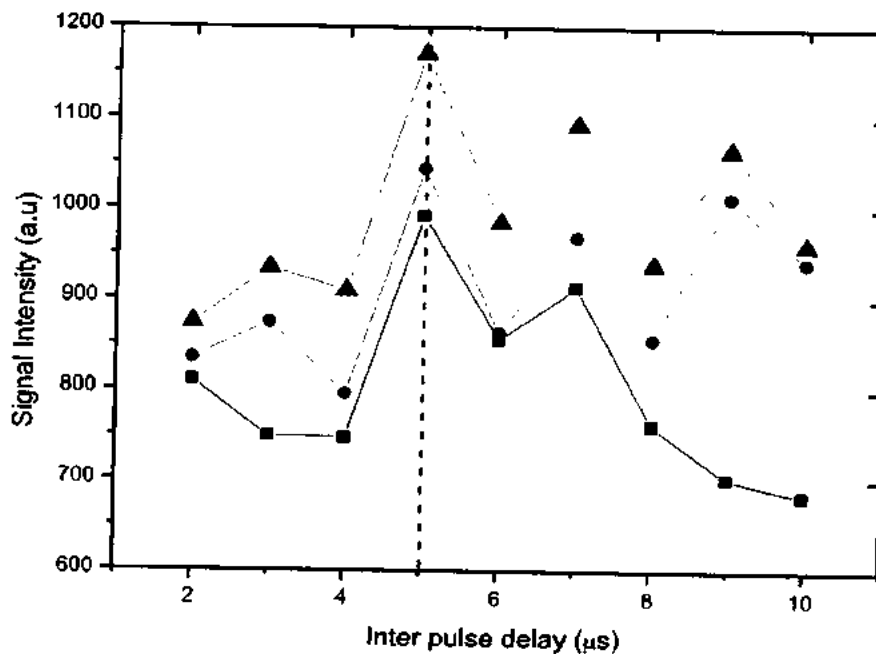


*Figure 3.4 Variation in signal intensities of three lines at 308.24 nm, 358.7 nm, 394.4 nm with inter pulse delay.*

## Experimental Results and Discussion

### Effect of laser pulses energy ratio

In double pulse LIBS, the energy ratio of the two laser pulses has important role in signal enhancement. Setting the inter pulse delay at 5 microseconds, the energies of the laser pulses has been varied in a way that total energy remained fixed.

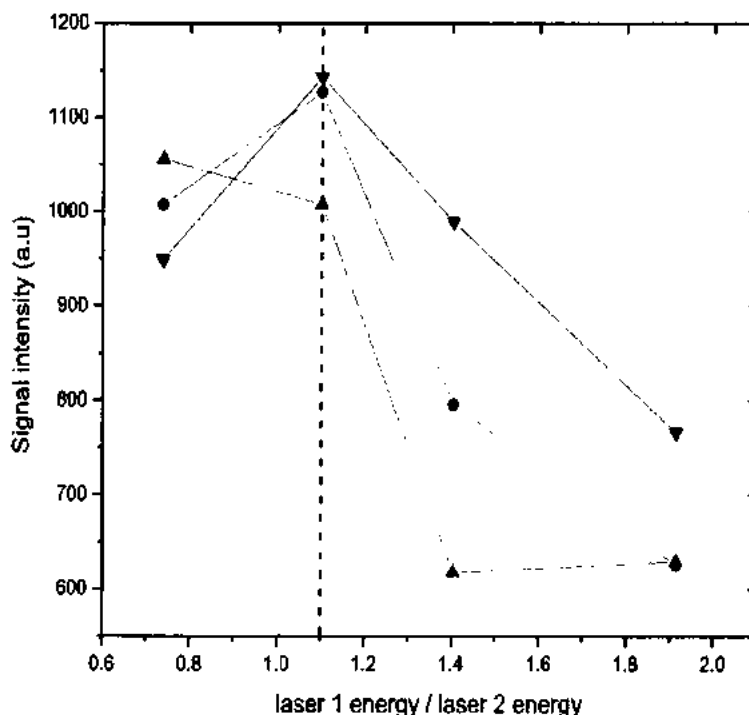


*Figure 3.5 Variation in signal intensity as a function of energy ratio.*

The emission spectra of polymer were recorded at different energy ratio ranging from 0.6 to 2.0. Fig. 3.5 shows the variation in signal intensities of three emission lines with respect to change in energy ratio of the laser pulses. It is evident from the figure that signal intensities are low at energy ratio 0.8, which increases to maximum at 1:1 energy ratio and thereafter again decreases. Thus the maximum enhancement in the emission spectra of polymer is observed at 5 microseconds inter-pulse delay and 1:1 energy ratio of the two laser pulses.

Under these optimized parameters, the emission spectra have been recorded in collinear geometry as shown in Fig. 3.6. This figure shows enhanced emission spectra as compared to single pulse spectra with same total energy. All the emission lines were observed as was detected in single pulse but with higher intensities.

## Experimental Results and Discussion

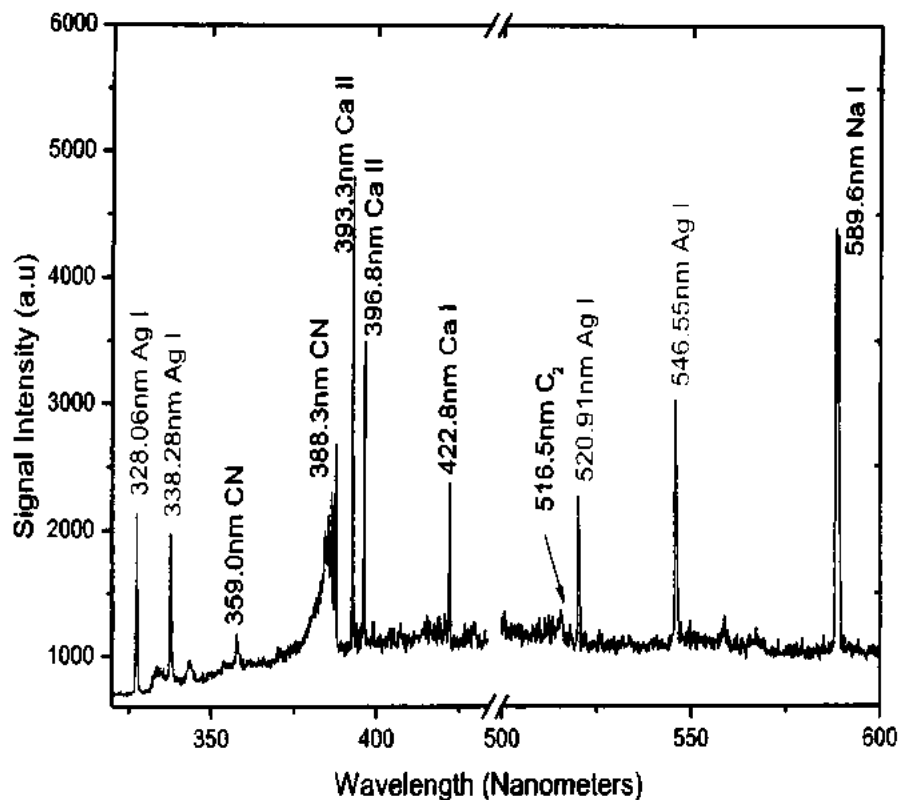


*Figure 3.6 Double pulse emission spectra of polymer.*

The comparison of single and double pulse LIBS spectra of silver doped polymer show that the emission lines of silver and calcium enhanced many times but the emission intensities of sodium lines is lower than the single pulse. This kind of behavior is reported by Gautier et al [42] in neutral lines of Mn (403.30 nm) and Al (306.43 nm). They observed that that this behavior is independent of the gate delay. Narayanan et al [43] also reported 30 times emission enhancement in silicon lines and 100 times in aluminum in double pulse LIBS with same total energy of single pulse. The possible reasons for this behavior include different excitation energies for different elements and lines and binding with other species in a sample [44].

Figure 3.7 shows the enhancement in peak intensity by comparing single and double pulse spectra in the range 332-342 nm. The silver emission line at 338.28 nm shows five times enhancement in double pulse signal intensity, which may be attributed to more plasma generation and enhanced material ablation. Expanded plasma size and increased material exclusion also causes enhancement in signal intensity as indicated by Noll et al. [45]. The enhancement in signal intensity due to double pulse is described by several groups [46,47]. Forsman et al. [48] explained

## Experimental Results and Discussion

the enhancement mechanism, firstly, the energy of second pulse is absorbed by ejecta from first pulse and target surface is affected by heated ejecta. Second pulse is the heat source which contacts through heating of ejecta. So that material removal progress efficiently. Furthermore, double pulse enhancement factors include ion yield, ion kinetic energy, plasma temperature, electron density, size and shape of plasma plume, lifetime of plasma, particles or nanoparticles generation.

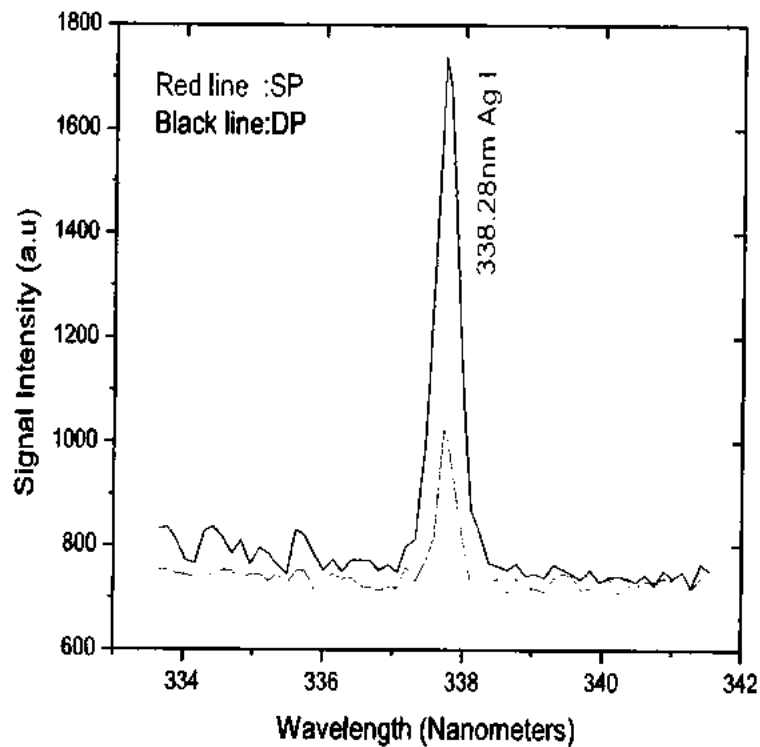


*Figure 3.7 Comparison of signal intensity on using single and double pulse.*

### 3.2 Calibration Curves

Calibration curve is the plot of signal intensity of the emission line of an element versus elemental concentration present in a sample. The linear fitting over the data points gives slope and intercept which can be used for the quantitative analysis and for the determination of limit of detection. The slope of the calibration curve is the measure of sensitivity of LIBS instrument. The sharp slope of the curve means that the calibration curve is more sensitive, whereas the nonlinearity is generally appears due to the saturation in line intensity and this portion is least sensitive in terms of




## Experimental Results and Discussion

---

quantitative measurements. It is therefore recommended that use the linear portion of the calibration curve to get reliable data for the unknown analyte.

In the present work, in order to construct calibration curve, polymers samples of different concentration of silver nitrate have been prepared. The detail of sample preparation is described in chapter 2. Briefly, twelve samples of known concentration of silver nitrate doped polymer, ranging from 1000 to 0.24  $\mu\text{g}$  as listed in table 3.1 were irradiated with intense laser pulse. The plasma has been generated on the surface of each sample under identical experimental conditions and the associated emission spectra have been analyzed. The emission intensities of silver lines at 328.06 nm, 338.28 nm, 520.91 nm, and 546.55 nm have been plotted as a function of concentration.

*Table 3.1 composite and percentage concentration of reference samples is given below.*



1	1000
2	500
3	250
4	125
5	63
6	31
7	16
8	8
9	4
10	2
11	1
12	0.30

Calibration curves have been constructed using above samples from 1000 to 0.30  $\mu\text{g}/\text{ml}$  using single and double pulse as shown in figure 3.8.

## Experimental Results and Discussion

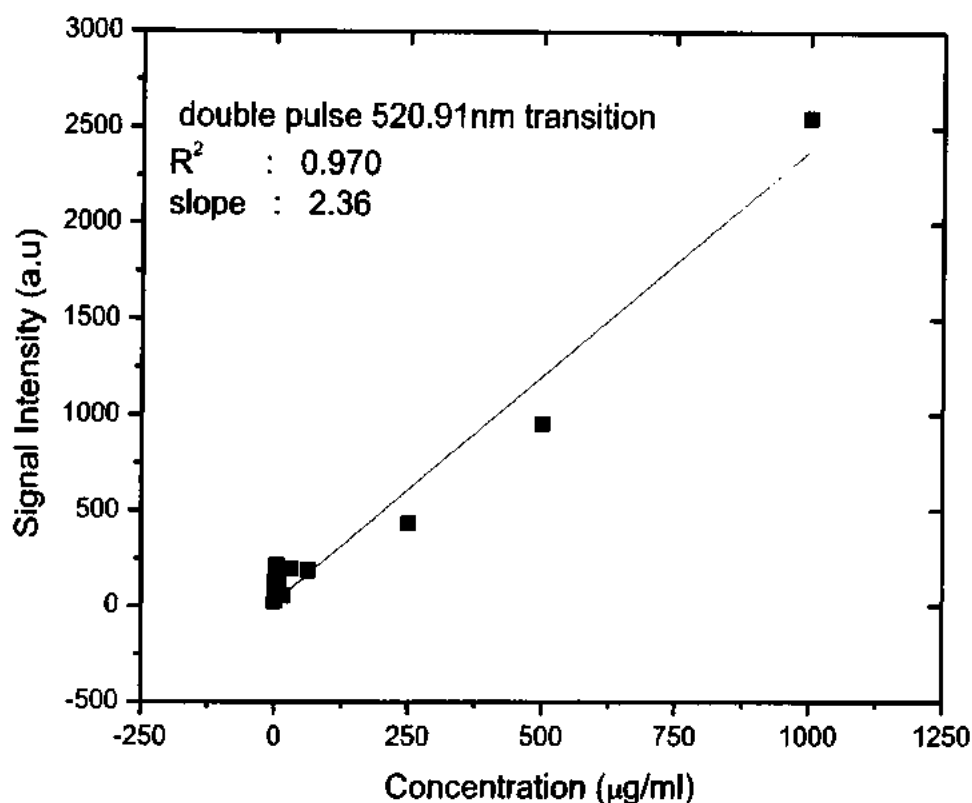


**Figure 3.8** Calibration curve showing all data points from 1000-0.30 µg/ml concentration of transition of Ag in polymer

Figure 3.8 shows the calibration curve between the concentration of Ag and intensity of the silver peak at 520.91 nm. It is clear from the graph that for the lower concentration region points are so close that they overlap. We cannot determine the correct slope from this graph. As to find the limit of detection, the lower concentration region is important so we have drawn the calibration curve for the low concentration region in figures 3.9 (a) and (b) for SP.

Fig. 3.9 (a and b) are the graphs of calibration curve using emission intensities of silver lines at 328.06 nm and 546.55 nm. Figure 3.9 (a) shows an increasing intensity (solid squares) with concentration of silver in polymer as indicated by linear curve fitting (solid red line). The good correlation factor close to unity shows that linear fit is a good representative of the experimental data.

## Experimental Results and Discussion

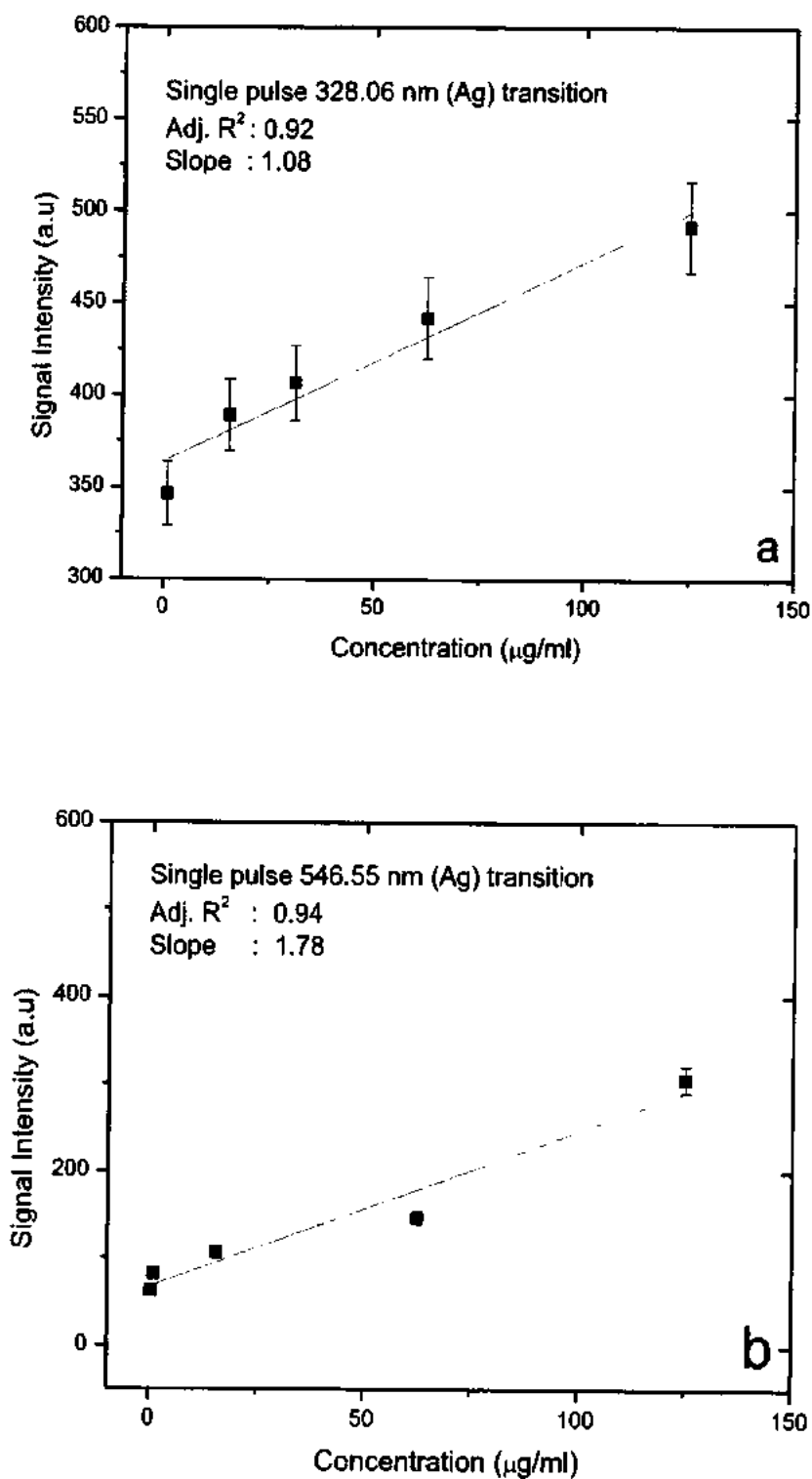


**Figure 3.9** (a and b) show calibration curves of Ag transition (328.06 nm and 546.55 nm) in polymer using single pulse

## Experimental Results and Discussion

---

The error bars represents deviation of data points from the linear fit, which is 5 % at maximum. Similarly, the emission intensities of silver line at 546.55 nm have been used for the construction of calibration curve. Figure 3.9 (b) represents the calibration curve with linear fitting which yield slope 1.30 and adjusted  $R^2$  value 0.90. Correlation coefficient, although not very close to unity but still fairly represent the data with 5 % uncertainty in fitting. The slope extracted from both the calibration curves is used for the extraction of limit of detection, which is a measure of sensitivity of the system.

The experiments were performed using double pulse arrangement in collinear geometry. The experimental conditions were kept same as that for single pulse LIBS. LIBS system was externally triggered and optimized for double pulse. Inter-pulse delay was fixed at 5 $\mu$ s and energy ratio was set at 1:1. Under these arrangements, the emission spectra have been recorded for different samples of silver doped polymer. In this configuration, it was observed that signal intensity get enhanced many times as compared to single pulse LIBS. These enhanced emission intensities have been used for the calibration curves. In figure 3.10(a) calibration curves of silver transition at 328.06 nm was constructed by plotting signal intensity as a function of concentration of different polymer samples. Applying linear fitting on all data points which gives the value of correlation coefficient and slop. Correlation coefficient value must be close to unity which shows all data points lie on the linear fitting. Deviation of data points from the linear fit, which is 5% at maximum. Similarly, calibration curves for 328.06 nm, 520.91 nm and 546.55 nm were constructed as shown in figure 3.10 (b), (c) and (d) respectively. The slopes from these calibration curves as listed in table 3.3 were used for the determination of limit of detection.

## Experimental Results and Discussion

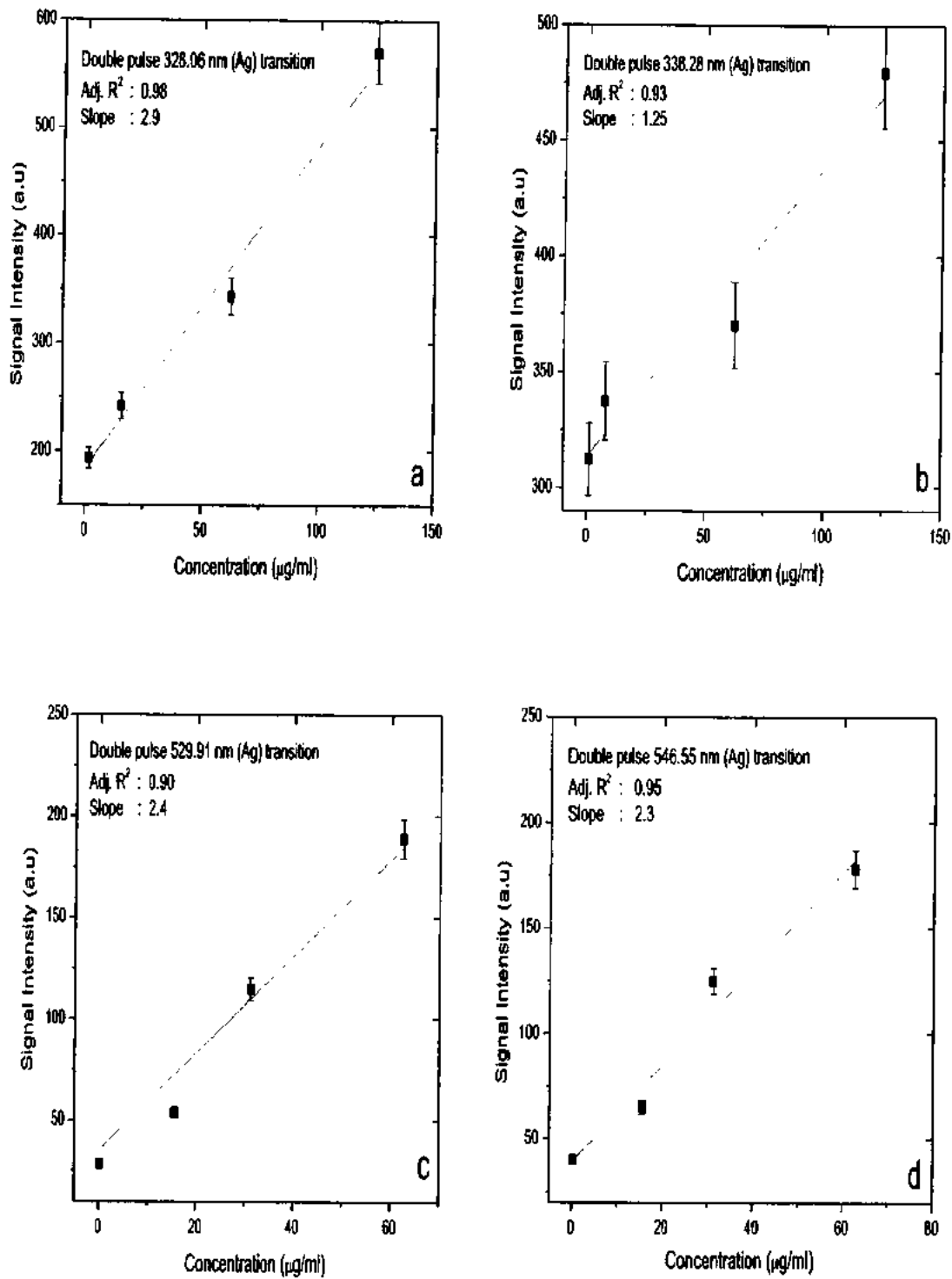


**Figure 3.10** (a-d) shows calibration curve of silver transition at 328.06 nm, 338.28 nm, 529.91 nm and 546.55 nm respectively, acquired using double pulse LIBS.

### 3.3 Limit of detection

Limit of detection (LOD) is a measure of the minimum quantity of any specie in a sample that can be detected by the experimental setup used. It is a measure of the analytical sensitivity by which extant the system capable to detect the trace or ultra-trace species. The LOD becomes more important when dealing with trace and ultra-trace quantification of the species. In spectroscopy, the limit of detection can be determined as follows.

$$LOD = \frac{3s}{b} \quad (3.1)$$

Where  $s$  is the standard deviation of background, taken from blank sample for each transition and  $b$  is the slope of the calibration curve. The slope is already extracted from the calibration curve, whereas the standard deviation is determined from the emission spectra of blank sample. The blank sample has been irradiated by an intense laser beam and the plasma has been generated on the surface of un-doped polymer. This experiment has been repeated many times and each time the emission spectra were collected and analyzed. We could not detect any emission lines of silver in the spectra. In order to get the standard deviation of blank sample, we used the signal intensity at a spectral position where silver lines would lie if it was present in a sample. Thus the signal intensity obtained from each spectra have been plotted as a function of number of observation in figure 3.11.

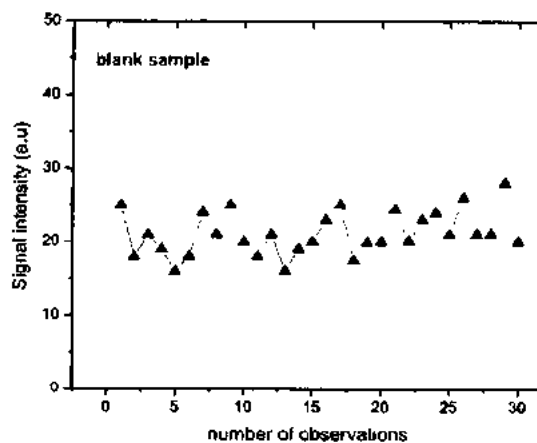


**Figure 3.11** Plot of signal intensities of the blank sample acquired at a spectral position of silver lines.

## Experimental Results and Discussion

Measuring the standard deviation of blank and slope of the calibration curve built from silver emission lines, we used these values in Eq. (3.1) and extracted the limit of detection for two silver lines 328.06 nm and 546.55 nm. The values of limit of detection together with slope of the calibration curves, standard deviation of blank and adjusted  $R^2$  are listed in table 3.2.

**Table 3.2** Values of limit of detection using single pulse LIBS and parameters extracted from calibration curves.

	328.06	0.92	7	1.08	19.50±1
	546.55	0.94	6	1.78	10.10±0.5

The limit of detection extracted using single pulse LIBS is 10 and 19  $\mu\text{g/ml}$ , which means that in single pulse LIBS set up we can detect the elements having 10 and 19  $\mu\text{g/ml}$  or more concentration in a sample. Aguilera et al. [21] determine carbon contents in steel by focusing laser pulse of 200 mJ in nitrogen atmosphere, obtained limit of detection 65 ppm with precision of 1.6 %. Marva et al. [25] investigate limit of detection for different element in aluminum and steel alloy at atmospheric pressure at energy 120 mJ using single pulse. Marva et al. [26] study matrix effect in limit of detection and limit of detection of Mg, Si, Mn and Cu as trace element was found in aluminum standard samples alloys using single pulse by focusing 70 mJ of laser pulse at 1064 nm with 7 ns duration and compare it with the values of same elements in steel alloys. Jurak et al. [27] performed experiment in vacuum ultraviolet range (UVU,  $\lambda < 200 \text{ nm}$ ) for detection of trace element in polyethylene (PE), at energy 50 mJ and pulse repetition rate of 10 Hz and obtain limit of detection 50  $\mu\text{g/g}$  for sulphur and 215  $\mu\text{g/g}$  for zinc.

The LOD values determined using single pulse LIBS is not very good and with this setup we cannot detect ultra-trace species in a sample. Therefore, to improve the limit of detection, double pulse LIBS is used [49]. The application of double LIBS, improve the system sensitivity many times as compared to single pulse LIBS and subsequently the limit of detection.

### Improvement in limit of detection using double pulses

The double pulse LIBS has been applied to detect and quantify the trace and ultra-trace species in a sample. The double pulse LIBS is the best choice for this purpose. Double pulses from two different laser system were utilized and the inter pulse delay and energy ratio were optimized as described previously. Under these optimized conditions the emission spectra of reference samples (silver doped polymer) and blank polymer have been recorded. The recorded spectra of silver doped polymer is shown in figure 3.6 and that of blank sample is shown in figure 3.12. The emission spectra of blank show that there is no emission lines of silver at a spectral position where it should be if the silver was present in a sample. Thus this spectra has been used for the determination of standard deviation of blank.

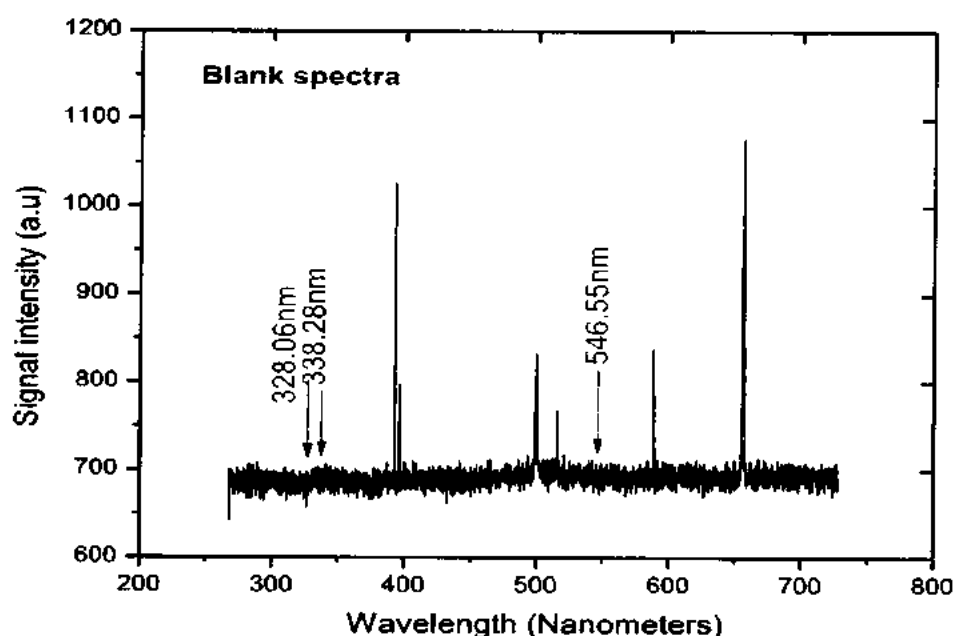


*Figure 3.12 Emission spectra of blank sample showing no transition line at 328.06, 338.28, 520.91 and 546.55 nm (Ag lines).*

The recorded spectra were analyzed and the calibration curves were built using silver emission lines (see Fig 3.10). The emission spectra of blank (un-doped) polymer were used for the determination of standard deviation of blank sample in a way describe earlier. The slope of calibration curve and standard deviation of blank sample have been used in equation 3.1 and limit of detection (LOD) have been extracted as listed in table 3.3. This time we have used four emission



## Experimental Results and Discussion

lines of silver and extracted LOD values approximately 6 µg/ml. These values are significantly lower than single pulse case. This improvement in LOD may be attributed to better laser plasma coupling and increased interaction volume which made the system more sensitive than single pulse LIBS. Marva et al. [25] investigated limit of detection of different elements in standard aluminum and steel sample using single and double pulse collinear configuration at atmospheric pressure. They reported up to ten times improvement in limit of detection for Ti, which is much higher than the present work. In the present work we improved limit of detection about two times using silver emission lines. Jiang et al. [50] investigated limit of detection using sulphur and carbon lines in steel sample using double pulse technique. The ratio of limit of detection of single and double pulse can be expressed as follows:

$$\alpha = \frac{LOD_{SP}}{LOD_{DP}} \quad (3.2)$$

The value of  $\alpha$  signifies the improvement factor due to double pulse and the higher ratio means improved sensitivity. It is observed that the LOD obtained in double pulse arrangement is approximately double than single pulse LIBS.

**Table 3.3** Chosen emission lines and their spectroscopic data for various elements is given for double pulse.

	328.06	0.98	5.3	3.0	5.3±0.3
	338.28	0.93	2	1.25	4.8±0.24
	520.91	0.90	4	2.4	5.0±0.25
	546.55	0.95	5	2.3	6.55±0.3

### 3.4 Study of plasma parameters

The radiations emitted from the laser induced plasma can be used to get knowledge of plasma through plasma parameters such as electron temperature and electron number density. These parameters help us to study plasma condition in time and space, which is helpful in fundamental understanding of the plasma. The commonly used optical emission spectroscopic methods for the determination of plasma temperature are the intensity ratio method, Boltzmann plot method and

## Experimental Results and Discussion

Saha-Boltzmann plot method, whereas electron number density is extracted using Stark broadening in line profile using equation 1.12.

### 3.4.1 Plasma temperature

In the present work, intensities ratio method has been used by assuming that plasma is optically thin and in local thermodynamic equilibrium. The integrated intensities ratio of emission lines which are well spaced, free from spectral interference and belong to same ionization stage have been used for the determination of electron temperature. The following expression is used for the estimation of plasma temperature.

$$\frac{I_1}{I_2} = \frac{g_1 A_1 \lambda_2}{g_2 A_2 \lambda_1} \exp \left[ - \left( \frac{E_1 - E_2}{kT_e} \right) \right] \quad (3.3)$$

Where I, g,  $\lambda$ , E are the intensity, statistical weight, wavelength and energy of transition line respectively. In the present work, two silver lines at 328.06 nm and 546.55 nm have been selected for the measurement of plasma temperature. The relevant spectroscopic data of these two lines are listed in table 3.4.

*Table 3.4 Spectroscopic data required for the determination of plasma temperature.*

Wavelength $\lambda$ (nm)	Transition	Statistical weight of upper state	Transition Probability A ( $10^7 s^{-1}$ )	Upper Energy Level ( $cm^{-1}$ )
	$4d^{10}5p^2p_{3/2} \rightarrow 4d^{10}5s^2S_{1/2}$	4	14	30472.66
	$4d^{10}5d^2D_{5/2} \rightarrow 4d^{10}5p^2P_{3/2}$	6	8.6	2907.96

The integrated emission intensities from the spectra and their data from literature have been used in equation 3.3 and the plasma temperature has been extracted as 10,000 K with 10 % uncertainty. This includes the uncertainty in transition probabilities and signal intensities. These findings are consistent with the reported work of Mussadiq et al. [51]. They reported the electron temperature of silver by Boltzmann plot method to be in the range of 17895 K to 10593 K as a function of energy of second harmonic of Nd: YAG laser.

## Experimental Results and Discussion

---

### 3.4.2 Electron Number Density

The electron number density in polymer plasma has been determined using stark broadened line profile of silver line ( $4d^{10} 5p \ ^2P_{1/2} \rightarrow 4d^{10} 5s \ ^2S_{1/2}$ ) at 328.06 nm. The FWHM of the line profile was extracted by fitting the following Lorentzian function over the line profile.

$$y = y_0 + \frac{2A}{\pi} \left( \frac{w}{4(x - x_c)^2 + w^2} \right) \quad (3.4)$$

Where

$w$  = full width half maximum (FWHM),

$x_c$  = central width,

$y_0$  = background emission

$A$  = Integrated area of emission line.

Figure 3.13 shows the Lorentzian fitting (red solid curve) over the data points. The FWHM of Ag (328.06 nm) line and the stark impact parameter from the list has been used in equation 3.5 and extracted the electron number density.

$$N_e = \left( \frac{\Delta\lambda_{1/2}}{2\omega} \times 10^{16} \right) \quad (3.5)$$

Where

$N_e$  = electron number density,

$\omega$  = electron impact parameter

$\Delta\lambda_{1/2}$  = FWHM of stark broadening line profile.

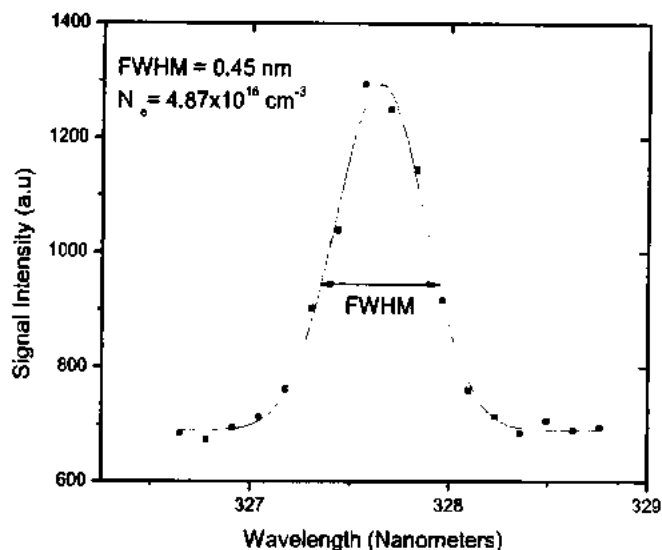


**Figure 3.13** Typical Silver emission line (328.06 nm), fitted with Lorentzian function.

In the present work, this technique has been used for the estimation of electron number density of silver doped polymer plasma. A typical line profile of Ag (328.06 nm), recorded at 1064 nm laser wavelength is shown in figure 3.13. The emission line has been fitted using Lorentzian function which yields its FWHM as 0.45 nm. Whereas the electron impact parameter was obtained from literature [52]. Using these parameters in equation 3.5, the electron number density has been estimated as  $4.87 \times 10^{16} \text{ cm}^{-3}$ . The uncertainty in the electron number density measurement is  $\sim 15\%$ , which include the uncertainties in the electron impact parameter, FWHM measurement and in the de-convolution of the line width to the instrumental width.

Similarly, electron number density using another silver line at 338.28 nm has been extracted as  $4.93 \times 10^{16} \text{ cm}^{-3}$ . Our measurement of electron number density are in good agreement with Jurak et al. [27]. They reported electron number density as a function of time ranging from 400 ns- 2 $\mu$ s as  $15 \times 10^{16} \text{ cm}^{-3}$  to  $3 \times 10^{16} \text{ cm}^{-3}$ . Mussadiq et al [51] also reported electron number density using 827.35 nm transition of silver as  $2.229 \times 10^{15}$  to  $6.44 \times 10^{14} \text{ cm}^{-3}$  at 17.6 mJ and  $1.76 \times 10^{16}$  to  $1.893 \times 10^{15} \text{ cm}^{-3}$  for 88.6 mJ energy.

### Conclusion

Laser induced breakdown spectroscopy (LIBS) technique has been used for analysis of emission spectra from the plasma generated by the fundamental harmonic (1064 nm) in air at atmospheric pressure using single and double pulse. Calibration curves have been plotted and limit of detection (LOD) has been determined of trace element (silver), which is in known concentrations, in polymer. With single pulse at 120 mJ, calibrations curves have been constructed and LOD determined as 10 and 19  $\mu\text{g/ml}$ . To improve sensitivity, double pulse configuration was used with inter-pulse delay at 5  $\mu\text{s}$  and energy ratio fixed at 1:1 and the LOD extracted as 7  $\mu\text{g/ml}$ . In addition, plasma parameters have been determined. Plasma temperature determined from intensity ratio method using transitions 328.06 and 546.55 nm as 10 000 K with uncertainty of 10 %. Electron number density has been observed from stark broadening using transitions 328.06 and 338.28 nm to be  $4.87 \times 10^{16} \text{ cm}^{-3}$  and  $4.93 \times 10^{16} \text{ cm}^{-3}$  respectively.

### Future Recommendations

In future, we will extend this work to investigate the limit of detection (LOD) using double pulse in orthogonal configuration. In this configuration first laser with low energy ablate the material and second laser re heat the plasma. This arrangement is considered as almost nondestructive.

## References

- [1] B. Kearton and Y. Mattley, "Laser induced breakdown spectroscopy", *Nature Photonics* **2**, 537 (2008).
- [2] D.A. Cremers and L.J. Radziemski, "Handbook of laser induced breakdown spectroscopy", Chichester Wiley, (2006).
- [3] US Army Research Laboratory, <http://www.arl.army.mil>
- [4] NIST Atomic Spectra Database, <http://physics.nist.gov>.
- [5] F. Brech and L. Cross, "Laser-Induced Breakdown Spectroscopy", *Appl. Spectrosc.* **16**, 59 (1962).
- [6] J. Debras-Guedon and N. Liodec, "Handbook of laser induced breakdown spectroscopy", *C.R Acad. Sci.* **257**, 3336 (1963).
- [7] P.D Maker, R. W. Terhune, and C. M. Savage, "Optical third harmonic generation", *Proceedings of Third International Conference on Quantum Electronics, Paris, Columbia University Press, New York*, **2**, 1559 (1964).
- [8] E. R. Runge, R. W. Minck and F.R. Bryan, "Laser-Induced Breakdown Spectroscopy", *Spectrochim. Acta B* **20**, 733 (1964).
- [9] R. H. Scott and A. Strashiem, "Laser induced plasmas for analytical spectroscopy", *Spectrochim. Acta Part* **25B**, 311 (1970).
- [10] N. R. Isenor, "Dissociation and breakdown of molecular gases by pulsed CO<sub>2</sub> laser radiation", *Appl. Phys. Letters* **18**, 224 (1971).
- [11] L. J. Radziemski and T.R. Loree, "Laser induced breakdown spectroscopy", *J. Plasma Chem. Plasma Process* **1**, 281 (1981).
- [12] D. A. Cremers and L. J. Radziemski, "Laser induced breakdown spectroscopy", *Anal. Chem.* **55**, 1252 (1983).

## References

---

- [13] D. A. Cremers, L. J. Radziemski and T.R. Loree, "Laser induced breakdown spectroscopy: Theory and Applications", *Appl. Spectrosc.* **38**, 721 (1984).
- [14] J. R. Wachter and D. A. Cremers, "Determination of Uranium in Solution Using Laser-Induced Breakdown Spectroscopy," *Appl. Spectrosc.* **41**, 1042 (1987).
- [15] D. A. Cremers, "Mobile beryllium detector (MOBEDEC) operating manual", Los Alamos National laboratory Los Alamos, NM Lasers-Induced Plasmas and Applications (1988).
- [16] D. E. Poulain and D. R. Alexander, "Laser Induced Breakdown Spectroscopy", *Appl. Spectrosc.* **49**, 569 (1995).
- [17] L. M. Cabalin and J. J. Laserna, "Experimental determination of laser induced breakdown thresholds of metals under nanosecond Q-switched laser operation," *Spectrochim. Acta. Part B* **53**, 723 (1998).
- [18] M. A. Ismail, H. Inam, Asmaa Elhassan, Walid T. Youniss and M. A. Harith, LIBS, "limit of detection and plasma parameters of some elements in two different metallic matrices", *J. Anal. At. Spectrom.* **19**, 489 (2004).
- [19] N. M. Shaikh, Y. Tao, R. A. Burdt, S. Yuspeh, N. Amin and M. S Tillack, "Spectroscopic studies of tin plasma using laser induced breakdown spectroscopy", *Journal of Physics* **244**, 42005 (2010).
- [20] E. R. Schenk and J. R. Almirall, "Elemental analysis of cotton by laser-induced breakdown spectroscopy", *Appl. Optics* **49**, 13 (2010).
- [21] J. A. Aguilera, C. Aragon, and J. Campos, "Determination of carbon content in steel using laser induced breakdown spectroscopy", *Appl. Spectrosc.* **46**, 1382 (1992).
- [22] J. Scaffidi, S.M. Angel and D.A. Cremers, "Emission enhancement mechanisms in dual-pulse LIBS", *Anal. Chem.* **78**, 24 (2006).
- [23] J. Pender, B. Pearman, J. Scaffidi, S.R. Goode and S.M. Angel, "Laser-induced breakdown spectroscopy using sequential laser pulses, *Laser Induced Breakdown Spectroscopy*", Cambridge University Press, Cambridge, UK, 516 (2006).

## References

---

- [24] X. Mao, X. Zeng, S. B. Wen and R.E. Russo, "Time-resolved plasma properties for double pulsed laser-induced breakdown spectroscopy of silicon", *Spectrochim. Acta Part B* **60**, 960 (2005).
- [25] M. A. Ismail, G. Cristoforetti, S. Legnaioli, L. Pardini, V. Pallaeschi, A. Salvetti, E. Tognoni and M. A. Harith "Comparison of detection limits, for two metallic matrices, of laser-induced breakdown spectroscopy in the single and double-pulse configurations", *Anal. Bioanal. Chem.* **385**, 316 (2006).
- [26] M. A. Ismail, H. Imam, A. Elhassan, W. T. Younis and M. A. Harith, "LIBS limit of detection and plasma parameters of some elements in two different metallic matrices", *J. Anal. At. Spectro.* **19**, 489 (2004).
- [27] Jurak Jasik, Johannes Heitz, Johannes D. Pedarnig, Pavel Veis, "Vacuum ultraviolet laser-induced breakdown spectroscopy analysis of polymers", *Spectrochem Acta Part B* **64**, 1128 (2009).
- [28] S. M. Angel, D.N. Stratis, K. L. Eland, T. Lai, M.A. Berg, and D.M. Gold, *Fres. J.*, "Laser induced breakdown spectroscopy", *Anal. Chem.* **369**, 320 (2001).
- [29] X. Jiang, P. Hayden, J. T. Costello and E. T. Kennedy, "Double-pulse laser induced breakdown spectroscopy with ambient gas in the vacuum ultraviolet: Optimization of parameters for detection of carbon and sulfur in steel", *Spectrochem. Acta Part B* **101**, 106 (2014).
- [30] LI Hong-Kun, LIU Ming, C. Zhi-jiang, L. Run-Hua, "Quantitative analysis of impurities in aluminum alloys by laser-induced breakdown spectroscopy without internal calibration", *Trans. Nonferrous Met. Soc. China* **18**, 222 (2008).
- [31] C. Lozep Moreno, K. Amponsah-Manager, B. W. Smith, I.B. Gornushkin, N. Omenetto, S. Palano, J. J. Laserna and J.D. Winefordner, "Quantitative analysis of low-alloy steel by microchip laser induced breakdown spectroscopy", *J. Anal. At. Spectrom.* **20**, 552 (2005).
- [32] T. L. Thiem, R.H. Salter, J. A. Gardner, Y. I. Lee and J. Sneddon, "Quantitative simultaneous elemental determinations in alloys using laser induced breakdown spectroscopy (LIBS) in an Ultra-High Vacuum", *Appl. Spectrosc.* **48**, 58 (1994).
- [33] A. P. Thorne "Spectrophysics" 2<sup>nd</sup> Ed. Champan and Hall, London (1988).



## References

---

- [34] X. Hou, L. Pan, Y. Sun, Y. Li, Y. He and H. Qi, "Study of the plasma produced from laser Ablation of a LBO crystal", *Appl. Surf. Sci.* **227**, 325 (2004).
- [35] H.C. Liu, X.L. Mao, J.H. Yoo, and R.E. Russo, "Early phase laser induced plasma Diagnostics and mass removal during single-pulse laser ablation of silicon", *Spectrochim. Acta Part B* **54**, 1607 (1999).
- [36] Mc Whirter RWP. "Spectral intensities", In: Huddleston R.H., Leonard S.L. Eds., *Plasma Diagnostic Techniques*, Academic Press, New York 1965.
- [37] Y. Godwal, S.L. Lui, M.T. Taschuk, Y.Y. Tsui, R. Fedosejevs, "Determination of lead in water using laser ablation-laser induced fluorescence", *Spectrochimica Acta Part B*, **62**, 1443, (2007).
- [38] Sylvain Gregoire, Marjorie Boudinet, Frederic Pelascini, Fabrice Surma, Vincent Detalle, Yves Holl, "Laser-induced breakdown spectroscopy for polymer identification", *Anal bioanal chem.* **400**, 3331 (2011).
- [39] R. Sattmann, I. Monch, H. Krause, R. Noll, S. Couris, A. Hatziapostolou, A. Mavromanolakis, C. Fotakis, E. Larrauri and R. Miguel, "Laser- induced breakdown spectroscopy for polymer identification", *Appl. Spectros.* **52**, 456 (1998).
- [40] R. Ahmed and M.A. Baig, "A comparative study of single and double pulse laser induced breakdown spectroscopy", *J. Appl. Phys.* **106**, 033307 (2009).
- [41] S. M. Angel, D.N. Stratis, K. L. Eland, T. Lai, M.A. Berg, and D.M. Gold, "LIBS using dual- and ultra-short laser pulses", *J. Anal. Chem.* **369**, 320 (2001).
- [42] Gautier, "Study of the double-pulse setup with an orthogonal beam geometry for laser-induced breakdown spectroscopy", *Spectrochim. Acta Part B*, **59**, 975 (2004)
- [43] V. Narayanan and R.k. Thareja, "Emission spectroscopy of Laser-Ablated Si Plasma related to Nanoparticle Formation", *Appl. Surf. Sci.* **222**, 382 (2004).
- [44] Rizwan Ahmed and M. A. Baig, "On the optimization for enhanced dual-pulse laser-induced breakdown spectroscopy", *IEEE Transactions on Plasma Science* **38**, 2052 (2010).

## References

---

- [45] R. Noll, R. Sattmann, V. Sturm and S. Winkelmann, "Space- and time-resolved dynamics of plasmas generated by laser double pulses interacting with metallic samples", *J. Anal. At. Spectrom.* **19**, 419 (2004).
- [46] F. Colao, V. Lazic, R. Fantoni and S. Pershin, "A comparison of single and double pulse laser-induced breakdown spectroscopy of aluminum samples", *Spectrochim. Acta Part B* **57**, 1167 (2002).
- [47] J. Scaffidi, S.M. Angel and D.A. Cremers, "Emission enhancement mechanisms in dual-pulse LIBS", *Anal. Chem.* **78**, 24 (2006).
- [48] A.C. Forsman, P.S. Banks, M.D. Perry, E. M. Campbell, A.L. Dodell and M. S. Armas, "Double-pulse matching as a technique for the enhancement material remove rates in laser machining of metals", *J. Appl. Phys.* **98**, 1 (2005).
- [49] V.I. Babushok, F.C. Delucia Jr., J.L. Gottfried, C.A. Munson and A.W. Miziolek, "Double pulse laser ablation and plasma: Laser induced breakdown spectroscopy signal enhancement", *Spectrochim. Acta Part B* **61**, 999 (2006).
- [50] X. Jiang, P. Hayden, J. T. Costello and E. D. Kennedy, "Double-pulse laser induced breakdown spectroscopy with ambient gas in the vacuum ultraviolet: Optimization of parameters for detection of carbon and sulfur in steel", *Spectrochim. Acta Part B* **101**, 106 (2014).
- [51] M. Mussadiq, N. Amin, Y. Jamil, M. Iqbal, M. A. Naeem and H. A. Shahzad, "Measurement of electron number density and electron temperature of laser-induced silver plasma", *International J. of Engineering and Tech.* **2**, 32 (2013).
- [52] M. S. Dimitrijevic, S. Sahal-Brechot, "Stark broadening of AgI spectral lines", *Atomic Data and Nuclear Data Tables* **85**, 269 (2003).

## **Vitae**

The author of this thesis Ayesha Mahmood belongs to the District Rawalpindi. By the grace of ALLAH she passed her matriculation with first division from Quaid -e- Azam International School Rawalpindi in 2006. She passed her higher secondary examination, in ICS, in 2008. She did B.Sc. (Physics, Math, and Computer Science) in 2010 from University of the Punjab. She had done M.Sc. in Physics in 2012 from University of Wah, Wah Cantt. She became enrolled at IIUI in 2013. She completed her research project from National Institute of Laser & Optronics (NILOP). This manuscript is for the partial fulfillment of the degree of MS Physics.

